Fear and foraging in the ecosystem size spectrum generate diversity in fish life histories

Kindsvater, Holly K.[1], Juan-Jordá, Maria-José[2,3], Dulvy, Nicholas K.[2], Horswill, Cat[4,5,6], Matthiopoulos, Jason[7], Mangel, Marc[8,9]

1. Dept. of Fish and Wildlife Conservation, Virginia Polytechnic Institute and State University, 310 W. Campus Dr., Blacksburg, VA 24061, USA
2. Earth to Ocean Research Group, Dept. of Biological Sciences, Simon Fraser University, Burnaby, BC V5A 1S6 Canada
3. AZTI, Marine Research, Basque Research and Technology Alliance (BRTA). Herrera Kaia, Portualdea z/g, 20110 Pasaia – Gipuzkoa, Spain.
4. ZSL Institute of Zoology, Regent's Park, London, NW1 4RY, UK
5. Centre for Biodiversity and Environmental Research, Department of Genetics, Evolution and Environment, University College London, Gower Street, London, WC1E 6BT, UK
6. Department of Zoology, University of Cambridge, Downing St, Cambridge CB2 3EJ, UK
7. Institute of Biodiversity, Animal Health and Comparative Medicine, Graham Kerr Building, University of Glasgow, Glasgow, G12 8QQ, Scotland.
8. Theoretical Ecology Group, Dept. of Biology, University of Bergen, Bergen 5020, Norway
9. Institute of Marine Sciences and Dept. of Applied Mathematics and Statistics, University of California, Santa Cruz, CA 95064, USA.

Abstract

Understanding how fish growth and reproduction will adapt to changing environmental conditions is a fundamental question in evolutionary ecology. Studies focused on the physiological effects of climate change upon life histories and population demography often ignore size-dependent foraging and risk of predation. We embedded a state-dependent energetic model in an ecosystem size spectrum to model prey availability (foraging) and risk of predation (fear) experienced by individual fish as they grow. We examined how spectrum richness and temperature interact to shape growth, reproduction, and survival; we found that richer spectra led to larger body sizes, but effects of temperature on body size were relatively small. We applied our model to scenarios corresponding to species representing the three ecological lifestyles (ecotypes) of tunas, in some cases including seasonal variation in conditions. We predicted realistic patterns of growth of tunas and found that seasonality in resource accumulation and compression of reproduction into short time periods favors growth to larger body sizes. Our framework for predicting emergent life histories combines direct and indirect effects of productivity (foodscapes), individual risk (fearscapes), and metabolic processes and offers a promising approach to understand fish life history responses to changing ocean conditions.

Keywords – Body size evolution, energy budgets, metabolic theory, size spectra, state-dependent models, temperature-size rule, global climate change

Introduction

Correlations between increased temperature and decreased body size have been documented for a variety of species (Gillooly et al. 2001, Kingsolver and Huey, 2008). The body sizes and population biomasses of aquatic species are adapting rapidly to human-induced environmental change (Oke et al. 2020), motivating the need for biophysical models to predict growth and reproduction in changing environmental conditions (Cheung et al. 2008, Cheung et al. 2010, Blanchard et al. 2012, Fernandes et al. 2020). Beyond thermal physiology, the evolutionary consequences resulting from changing ecosystem productivity (foodscapes) and predator abundance (fearscapes) are difficult to disentangle from the effects of environmental temperature or seasonality on growth and related life history traits (Daufresne et al. 2009, Audzijonyte and Richards 2018, Neubauer and Andersen 2019). Classic and recent advances predicting optimal growth and reproduction of harvested populations (Holt 1958; Beverton and Holt 1959; White et al. 2022) have been combined with size-structured community interactions to predict the evolution of life history traits in specific taxa (Shuter et al. 2016). This approach provides a promising foundation for predicting ecological and evolutionary responses to climate change. While specific taxa within an ecosystem will adapt according to contextual factors such as phylogenetic lineage, adaptive capacity, and environmental variability, models incorporating the roles of food and fearscapes, seasonality, and other metabolic processes could explain adaptive variation among closely related taxa and refine our mechanistic understanding of species' responses to changing climate conditions (Free et al. 2019).

Research on life-history evolution has shown that in ectothermic species such as fish, increased risk of predation and food availability both can select for earlier ages at maturation and more

frequent reproduction, but that growth rates can be slower or faster depending on the interaction between body size, predation, and per-capita resource availability (Conover and Munch 2002; Walsh and Reznick 2009, Hulthén et al 2021). Within and between ectothermic species, development at higher temperatures can lead to smaller body sizes (Kingsolver and Huey 2008). Well-established theory addresses how trade-offs among these life-history traits determines individual body sizes and population demographic rates (Beverton and Holt 1959, Gadgil and Bossert 1970, Kozlowski 1992, Kozlowski 1996), but theory addressing the interacting effects of temperature and seasonality on growth is still developing (Varpe 2017). There is longstanding interest in the mechanisms leading to biphasic (or asymptotic) growth patterns predicted by the von Bertalanffy equation (Quince et al. 2008), as early models are based on simplistic assumptions (Audzijonyte et al. 2022). These growth models struggle to explain latitudinal and temporal trends in body size within and among species of fish (Audzijonyte et al. 2020), suggesting that such models do not sufficiently capture the relevant physiological and ecological drivers of fish life histories.

The role of metabolic requirements in shaping growth trajectories has been given increasing attention (Jørgensen et al. 2016, Wong et al. 2021, White et al 2022). Physiological processes can vary with the environmental temperature experienced by organisms (Brown et al, 2004, Clarke and Johnston, 1999). The allometric scaling of metabolic costs in different temperature regimes (known as the Metabolic Theory of Ecology [MTE]; Gillooly et al. 2001) has been used to predict individual body size according to the benefits of growing large (to increase foraging success and avoid predation), balanced against the costs of increased metabolic overhead and diverting resources from reproduction to growth (Wong et al. 2021). More detailed models of

energetic allocation have linked variable environmental conditions to growth, reproduction, and longevity (Kozłowski and Teriokhin 1999, Cichoń and Kozłowski, 2000, Lika and Kooijman 2003, Jorgensen and Fiksen 2006, Ejsmond et al. 2010, Chapman et al. 2011, Audzij*o*nyte et al. 2022). Understandably, the results of these models depend on specific assumptions made regarding the relationship between resources, mortality, and individual size; no models have addressed how seasonality in environmental conditions and spawning opportunities drive emergent patterns of growth and longevity in the same model.

We hypothesize that including size-based community interactions, in addition to temperature, in energetic models will reduce the number of *ad hoc* assumptions regarding mass-based foraging success and risk of predation, allowing other environmental drivers such as overall ecosystem productivity, temperature, and seasonal variation in these processes to be evaluated. This approach could yield more realistic predictions of diversity in fish life histories, providing significant insights into the mechanisms that determine adaptive responses to changing environmental conditions.

In aquatic ecosystems, size spectra relationships are often used to represent community interactions, as they connect body size, trophic level, and abundance across species (Sheldon et al. 1977, Thygesen et al. 2005, Law et al. 2009, Sprules and Barth 2016, Christensen and Andersen 2011, Andersen et al. 2016, Andersen 2019). In a community size spectrum, flow of energy between trophic levels via consumption and predation rates are characterized by individual mass, instead of species' identity (Benoît and Rochet 2004, Blanchard et al. 2009, Andersen 2019). The key property of size spectra is that an individual's relative position (mass)

113 determines both its prey field (foodscape) and its risk of predation (fearscape). Individuals are
114 born small and grow through the size spectrum over their lifetime, consuming prey that are a
115 fraction of their own size. Furthermore, size-spectrum theory assumes the lower limit of prey
116 size preference depends on the profitability of the prey, and the upper limit depends on the
117 maximum gape size of the predator. These interactions could equally apply to interactions within
118 size-structured populations of the same species (i.e., cannibalism). Therefore, predation and
119 consumption rates determined by different areas under a size-spectrum curve could be used to
120 simultaneously characterize the mass-specific caloric resource availability (foodspace) and risk
121 of predation (fearscape) experienced by an individual as it grows (Benoît and Rochet 2004,
122 Giacomini et al. 2013, Shuter et al. 2016, Andersen 2019).
123
124 Here, we use an energetically based model combining size-dependent resources and risk of
125 predation (both derived from size-spectra) with size- and temperature-dependent physiological
126 requirements in an energetic model predicting the evolution of growth, maximum body size,
127 reproductive investment, and longevity in different environments. Allocation to growth,
128 reproduction, and maintenance in one month affects an individual's size, survival chances, and
129 resources for reproduction in the next. We define fitness as expected lifetime reproductive
130 success and determine its maximum value and the associated life history decisions using
131 stochastic dynamic programming (Clark and Mangel, 2000, Houston et al.1988, Mangel, 2015).
132 We examine general patterns in the life history evolution of fishes under different scenarios of
133 ecosystem productivity and environmental temperature.
134

We next investigate the evolution of growth, body sizes and reproductive patterns in tuna species in varying environments, including seasonally varying conditions. Tunas (Family *Scombridae*) exhibit a wide range of maximum body sizes (~ 40 cm - 400 cm), longevities (~ 4 - 41 years) and reproductive patterns (Juan-Jorda et al. 2013, Horswill et al. 2019). Tunas are epipelagic species found in temperate and tropical waters around the world's oceans with varying vertical, latitudinal and seasonal distributions and movements. Confronting the predictions of our model with data on the life history diversity observed in tuna species in different environmental conditions gives us insight into the mechanisms underlying fish life histories and improve our ability to predict their response to future climate scenarios. Where possible, we use values for physiological processes measured for tunas, but we also consider the sensitivity of these parameters to ensure generality of our results.

Methods

Using the size spectrum to infer per-mass rates of prey encounter and predation

Studies across many orders of magnitude find that the relationship between the numbers of organisms and individual mass w is a power function with a scaling parameter κ and an exponent λ, which has been empirically estimated to be close to -1 when mass is logarithmically scaled (Sheldon et al. 1972, Trebilco et al. 2013, Sprules and Barth 2016, Hatton et al. 2021)

$$N(w) = \kappa w^{\lambda} \tag{1}$$

The Sheldon size spectrum, which follows from Eq. 1, is the distribution of total ecosystem biomass $B(w)$ across body size classes, and is represented by $B(w) = N(w)w$. Based on evidence from multiple ecosystems (Sprules and Barth 2016), total biomass slowly decreases as

individual mass increases; in log-log space, the spectrum – as originally conceived (Sheldon et al 1972) and recently confirmed (Hatton et al. 2021) – is nearly flat. We consider this index of biomass to reflect whole-ecosystem productivity, as this representation of community size spectra is not normalized by individual mass (Sprules and Barth 2016). Since $N(1) = \kappa$, we view κ as a metric of ecosystem productivity. In a log-log plot of Eq. 1, the y-intercept is the natural log of κ.

Prior research suggests that this phenomenon of linear aquatic size spectra emerges from three size-dependent eco-physiological processes: (1) the encounter rate of predators and prey; (2) the preference of predators for prey of a given size; and (3) the limit to prey consumption imposed by the size of the predator's stomach (the predator-prey mass ratio; Benoît and Rochet 2004, Blanchard et al. 2017, Andersen 2019). Anderson (2019) derived a method to calculate the prey available to individuals of mass *w* by relating the productivity of a spectrum to empirical estimates of prey encounter rates, predator-prey mass ratios, and prey preferences. Following his rationale, we assume that the prey biomass available per month to an individual is a concave function of mass *w*, and scaled to be approximately three times the size spectrum productivity κ (Andersen 2019). The empirical estimates of physiological processes used to simplify this derivation are associated with a significant amount of variability among species within a size class (Andersen 2019). However, as a starting point we assume that as a baseline the per-period food available for an individual of mass *w* is represented by

$$B_{prey}(w) = 3\kappa w^{0.05} \tag{2}$$

This equation approximates the integral over the foodscape of prey biomass (in kg) available to an individual of mass *w* each month (Fig. 1A). The foodscape is therefore the total biomass available to the predator, and the range of sizes of prey that it takes. To address variability in the threefold scaling factor, we chose to vary κ in subsequent analyses, representing ecosystem level differences in productivity (abundance) or potentially differences among taxa.

We define the fearscape as an individuals' instantaneous risk of predation, integrated across sizes of potential predators. For gape-limited taxa like fishes, a predator's prey field depends on its encounter rate with prey in its preferred size range. This encounter rate (the clearance rate) is typically measured in units of volume per time, as aquatic species forage in a three-dimensional habitat (Kiørboe and Hirst 2014). Again, we follow Andersen (2019), and use an empirically estimated constant of 0.07 to characterize the scaling of prey vulnerability with its mass, which is based estimates of preference windows of predators and the volume of water each clears per month that come from empirical distributions of prey sizes in predator guts (Ursin 1973). We also define a coefficient *h,* which modifies the probability of consumption - how likely a predator is to capture the focal individual (based on its hunger level or capture efficiency) - and use the reported allometric exponent of -0.25 to represent how predation mortality scales with body size (Figure 1B; Eq. 2.22 in Andersen 2019). From these, Anderson (2019) integrates over the Sheldon spectrum and produces a relationship predicting the scaling of mortality risk for prey $\mu_p(w)$ per month:

$$\mu_p(w) = 0.07hw^{-0.25} \tag{3}$$

We convert this instantaneous rate to the probability escaping from predators during each month (Hilborn and Mangel 1997, Mangel 2006), so we can represent the probability an individual survives from one month to the next $\gamma_{pred}(w)$ as:

$$\gamma_{pred}(w) = e^{-\mu_p(w)} \tag{4}$$

The resulting annual mortality curves are in Fig. 1B.

Defining physiological costs that depend on temperature and body mass

We assume metabolic costs that increase with body mass and environmental temperature (Clarke 2006). We model individual costs $C(w, \tau)$ (in joules) as a function of temperature τ in Kelvin, following the general form introduced in the MTE (Gillooly et al. 2001):

$$C(w, \tau) = cw^{\theta} e^{\left(-E/k_B\tau\right)} \tag{5}$$

Evidence for the MTE suggests the activation energy E (the energy required for the reactions of respiration and other metabolic processes) does not vary appreciably among taxa (Bernhardt et al. 2018); Boltzmann's constant k_B also does not vary. The normalization coefficient c accounts for differences among taxonomic groups in the intercepts of the linear relationship that arise from second-order effects such as stoichiometry or respiratory surface areas (Bigman et al 2021). The slope of this relationship in log space, θ, is strikingly similar among taxa (Brown et al. 2004). We use a value for θ estimated from physiological studies on tunas (Table 1) but vary it in sensitivity analyses. Note that τ in Eq. 5 is Kelvin, but hereafter we discuss temperatures in units

226 of Celsius. We use this general formula for scaling of metabolic costs at different temperatures τ

227 to describe the monthly energetic expenses of an individual of mass w (Fig 1C).

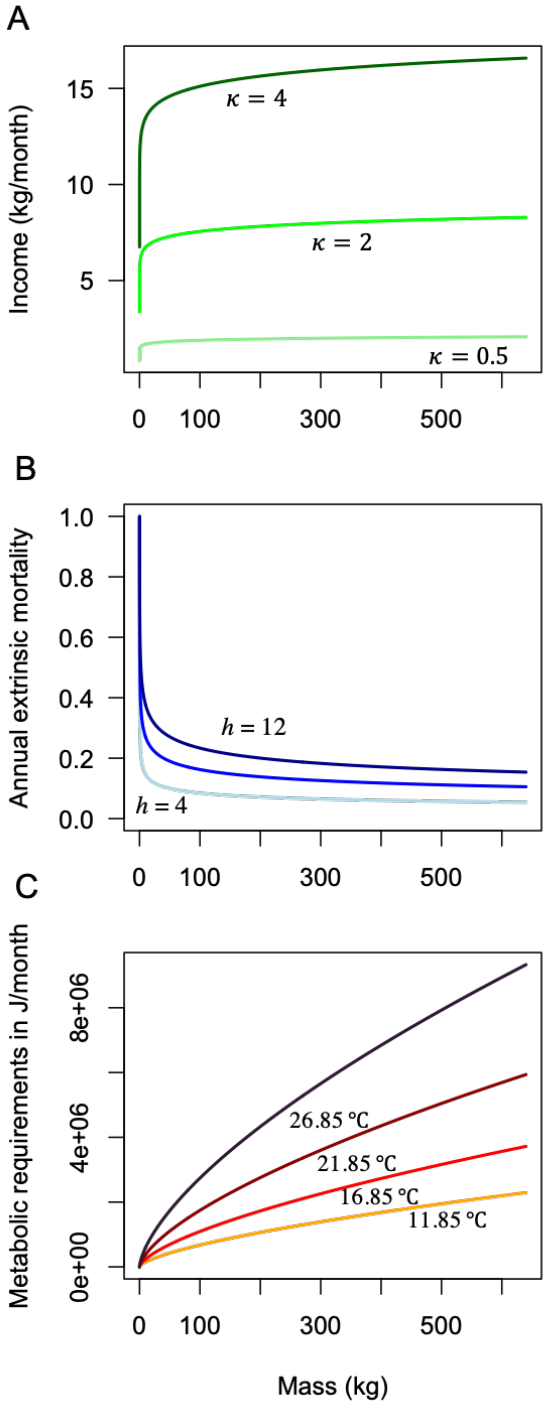

Figure 1. Examples of allometric relationships between individual mass and (A) income (in kg per month); (B) the scaling of predation with size and its interaction with predator efficiency (or hunger) h, and (C) metabolic costs, which also scale with temperature τ (on the graph, it is presented in degrees Celsius, °C; values used in Kelvin are 285, 290, 295 and 300K). Note that these curves represent a subset of values considered.

228

229 *Defining fitness and determining the optimal allocation strategy*

230 In Equations 2, 4, and 5, we define mass-specific food availability, predation risk, and costs,
231 allowing us to examine the variables influencing growth and reproduction in a common currency
232 of an individual's energy budget (Fig. 1). All parameters are defined and their values reported in
233 Table 1. To find the optimal life history strategy in different scenarios of ecosystem productivity
234 and temperature conditions, including seasonal variation, we developed a model of an
235 individual's energy budget, tracking two physiological state variables, the body length l and
236 energy (lipid) stores s of an individual, which vary dynamically over an individual's lifetime
237 (Fig. 2). Following the conventions for dynamic state-variable models, we denote the state
238 variables l and s are lowercase in the dynamic programming equation, representing the fact they
239 are iterated values. Later, when we refer to specific values of the state variables, we use
240 uppercase L and S.

241

242 We define fitness as expected lifetime reproduction, averaged over the stochastic process of
243 survival, which we calculate numerically using stochastic dynamic programming (Houston et al.
244 1988; Clark and Mangel 2000, Mangel, 2015). This method allows us to consider how individual
245 age and physiological state (energy stores and body length) affect the optimal trade-off between
246 growth and reproduction in the context of lifetime fitness. We assume that an individual allocates
247 a proportion of its budget to growth and reproduction on monthly time intervals. Our choice to
248 model allocation to growth and reproduction as proportions of an individual's energy budget
249 builds on prior dynamic state-variable models of fish growth (Jørgensen and Fiksen 2006,
250 Chapman et al. 2011).

251

Given specific values of $L(t)$ and $S(t)$, representing individual length and stores at the start of month *t,* we calculate structural mass $W(t)$ from length with a standard cubic function (Froese 2006):

$$W(t) = aL(t)^3 \tag{6}$$

and assume that only structural mass is relevant for size-dependent gains (B_{prey}) and costs (Fig. 2). We convert from mass to units of energy (joules) and back using a conversion factor estimated for tunas ($\rho = 4.2 \times 10^6$J/kg (Chapman et al 2011)) but that could take other values for other species. Each month, an individual acquires energy from food, determined by their structural mass *w* via Eq. 2. We then allow the individual to allocate proportions of its energy budget (which includes income and any stored energy) to growth (*g*) and reproduction (*r*).

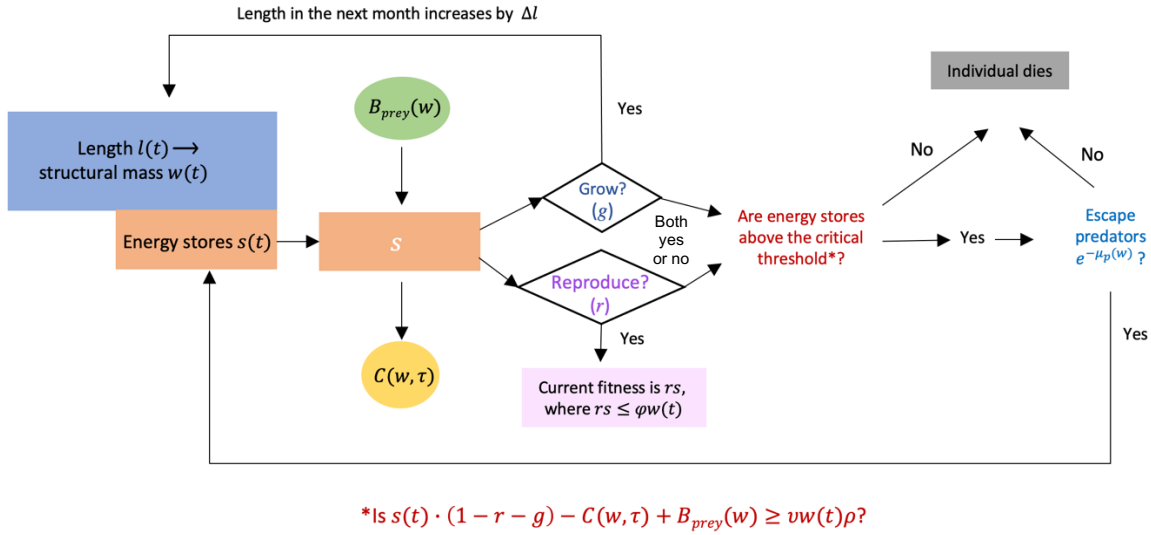

Figure 2. Schematic overview of the optimization algorithm calculating the two dynamically varying state variables, body length $l(t)$ and energy stores $s(t)$ within each month t, as well as current and expected fitness. Arrows represent the flow of energy or decisions. Round shapes represent inputs; rectangular shapes are model states and outputs (fitness and fate); diamonds are decisions. Note that $l(t)$ and $w(t)$ are related through Eq. 6. Both B_{prey} and μ_p are determined by the size spectrum. Survival to the next time step depends on (1) whether there is sufficient energy to allocate to growth and reproduction, pay costs, and exceed the critical threshold for lipid stores υ (which varies according to structural mass), and (2) the mass-dependent risk of predation μ_p.

Given an individual of with specific values for length $L(t)$ and energy stores $S(t)$, we calculate the increment of growth ΔL expected for each possible proportional allocation g. We convert this fraction of lipid stores from joules to the equivalent mass ($g\frac{S(t)}{\rho}$), and add it to existing mass,

such that $W(t+1) = W(t) + g\frac{S(t)}{\rho}$. We then calculate the new length by rearranging the mass-length relationship $W(t) = aL(t)^3$:

$$L(t+1) = \left[\frac{1}{a}\left(L(t)^3 + g\frac{S(t)}{\rho}\right)\right]^{1/3} \tag{7}$$

We repeat this for every possible combination of values of the state variables, *l* and *s.* For all $L(t) = l$ and $S(t)$ = s, we can determine the growth increment ΔL:

$$\Delta L(l, s, g) = \left[\frac{1}{a}\left(l(t)^3 + g\frac{s(t)}{\rho}\right)\right]^{1/3} - l \tag{8}$$

Values for proportional allocation of lipid stores to reproduction *r,* along with *g,* are combined to determine the dynamics of energy stores and length from one month to the next:

$$S(t+1) = B_{prey}(W(t)) - C(W(t), \tau) - (r+g) \cdot S(t)$$

$$L(t+1) = L(t) + \Delta L(L(t), S(t), g) \tag{9}$$

We assume that both stored energy and reproduction are limited by an individual's structural mass (which in turn depends on its length). These constraints represent limits on the amount of lipid that it is realistic to store, and mass of gametes that can be produced, given the capacity of the body cavity. If the proportions of energy allocated to reproduction and growth are less than 100% (meaning $r + g < 1$), the remaining energy is stored for future use, as long as total reserves do not exceed 60% of structural mass. This value is somewhat arbitrary but exploratory analyses suggest it does not have a strong effect on the results presented here because in practice individuals do not store their energy long enough to come close to exceeding this limit. Second,

we assume that reproductive output (in units of kg) is constrained so that it cannot exceed a fixed proportion of φ of structural mass $w(t)$, so that the following condition must be met:

$$\frac{rS(t)}{\rho} \leq \varphi w(l,t) \tag{10}$$

This size-based limit on total reproduction is used in the calculation of current fitness.

Current fitness

We let $R(r,s,l,t)$ denote the increment in fitness in month *t* when $L(t) = l$, $S(t) = s$, and a fraction of stores *r* is allocated to current reproduction. We model this constraint with an asymptotic function, such that the fitness increment increases smoothly toward the maximum possible for the given length *l(t):*

$$R(r,s,l,t) = \frac{rs}{1+({rs}/{\varphi w(l)})^f} \tag{11}$$

The asymptotic value of this function depends on the value of *f* in the denominator, which controls the abruptness of the constraint on current fitness (Supp. Fig. 1). In other words, the steepness of the multivariate landscape around the fitness optima is modulated by *f*. For simplicity, we assume $f = 1$ for all results presented hereafter. In that case,when $\varphi w(l,t) >> \frac{rs}{\rho}$, $R(r,s,l,t) \sim rs$ and when $rs >> \varphi w(l,t)$, then $R(r,s,l,t) \sim \varphi w(l)$.

Expected future fitness

At any age, expected fitness is determined by the sum of current reproduction and accumulated future reproduction, which is calculated assuming the individual behaves optimally at all future ages. This requires we calculate the future states (length and lipid stores) given each combination of allocation to growth and reproduction. We denote potential values of future states as $l'$and s'. In light of Eqs 7-11 these are

$$l'(l,s,g) = l + \Delta l(l,s,g)$$

$$s'(l,s,r,g) = B_{prey}\big(w(l)\big) - C(\,w(l),\tau) - (r+g)s \tag{12}$$

where $w(l)$ is the structural mass of an individual of length *l.* At the end of the month, if an individual's lipid stores fall below the critical threshold for its mass (its expenditures have exceeded its energy budget), it starves (Supp. Fig. 2). We let $\gamma_s(s,l)$ denote the probability of avoiding starvation in the current time and model it as

$$\gamma_s(s,l) = \frac{1}{1+e^{-q(s-\upsilon w(l)\rho)}} \tag{13}$$

involving two new parameters υ and q. The parameter υ determines the level of stores at which starvation begins and q is a shape parameter. When $s = \upsilon w(l)\rho$, the right-hand side of Eq. 13 is always ½. When q is large, then the right-hand side of Eq. 13 is approximately 1 when $s >$ $\upsilon w(l)\rho$ and 0 otherwise. Thus, this function specifies that if combined allocation to growth and reproduction causes an individual's lipid stores to decrease below the critical value for its mass the probability of survival decreases smoothly toward zero (See Supp. Fig. 2 for more details).

Equations 7-13 characterize changes in individual state and in fitness, given the possible monthly allocation strategies (*r* and *s*). With these functions in place, we can find the allocation strategy that maximizes current and future fitness at every age until the age of senescence or maximum lifespan, *T*, is reached (for all scenarios, we assumed the maximum lifespan of *T* = 216 months or 18 years). We define $V(l, s, t)$ as the maximum expected accumulated reproduction between time *t* and *T,* given size $L(t) = l$ and lipid stores $S(t) = s$. Since there can be no accumulated reproduction after *T,* we have the end condition $V(l, s, T) = 0$. Expected future fitness at every age $t < T$ is found by solving the stochastic dynamic programming equation

$$V(l, s, t+1) = \max_{g,r}\left[R(r, l, s, t) + \gamma_{pred}(w) \cdot \gamma_s(s, l) \cdot V\big((l'(l, s, g), s'(l, s, r, g), t\big)\right] \qquad (14)$$

The first term of the on the right-hand side of Eq. 14 represents reproduction in month *t*. The second term represents expected future reproduction, discounted by the probability of surviving predation $\gamma_{pred}\ (w)$ and starvation $\gamma_s(s, l)$, When these are combined, we obtain expected lifetime reproduction from time *t* onwards, given that size $L(t) = l$ and lipid stores $S(t) = s$.

The dynamic programming algorithm (Mangel and Clark 1988; Houston and MacNamara 1999) iterates over all viable combinations of *l* and *s,* at each time *t,* and stores the fitness of each allocation strategy. The optimal strategy (marked with an asterisk) at time *t* is the combination $g*$ and $r*$ associated with the greatest current and future fitness. Further details of the optimization algorithm are given in the Appendix. In Supp. Fig 3 we illustrate the array for both

358 allocation strategies ($g^*(l,s,t)$ and $r^*(l,s,t)$) at two ages, for all possible combinations of length
359 and lipid stores.
360
361 *Calculating the fate of individuals allocating optimally*
362 We used a Monte Carlo simulation to calculate the accumulating probability of mortality as an
363 individual ages, following the allocation rules generated by the solution of Eq. 14, which
364 provides optimal allocation rules for the range of state values specified in our numerical
365 algorithm. Some combinations of states (length, lipid stores and age) will not arise naturally and
366 others are inviable (the dark blue regions of Supp. Fig. 3). Therefore, to predict the relationships
367 between length, lipid stores, and age that will be observed in nature, we simulate the expected
368 fates of an individual that is born at a given size, and allocates energy according to the optimal
369 growth and reproduction fractions given by the solution to Eq. 14. We record the body length
370 and reproductive output in each subsequent month of an individual's life, and calculate its
371 probability of survival, given both the risk of starvation and the risk of predation. We use the age
372 past which the cumulative chance of survival is less than 3% as the expected lifespan. For
373 simplicity, we consider reproductive output in units of energy (joules) rather than considering
374 allocation to offspring size and number (Kindsvater et al. 2010); this can include migration costs.
375 We did not build in any assumptions about age at maturation, but rather let maturation patterns,
376 along with natural trade-offs between growth and reproduction (Supp. Fig. 3) emerge from
377 patterns of allocation.
378
379 *Scenarios for environmental variation*

380 We used our model to predict a range of fish life histories (growth, reproduction, and survival)
381 that are evolutionarily advantageous across different scenarios of ecosystem productivity and
382 environmental temperatures. To do this, we developed different productivity and temperature
383 scenarios corresponding to different conditions in the marine environment, and impose different
384 metabolic costs to individuals according to Eq. 5. We solved for the optimal life histories under
385 different temperatures (τ in Eq. 5 in units of Kelvin), converted to Celsius and ranging from
386 11.85 to 26.85 ℃ (285-300 K) in five degree intervals. We considered these temperature ranges
387 in different scenarios for ecosystem productivity, for which κ ranged from one to five. We
388 considered factorial combinations of these parameters to understand the implications of their
389 interactions for the evolution of fish life histories.
390
391 *Case study predicting life history diversity of tunas (Scombridae).*
392 We developed a case study for tunas to examine if our model can predict the general patterns of
393 life history variation in tunas. There are 15 species of tunas (Family *Scombridae*, genera
394 *Allothunnus*, *Auxis*, *Euthynnus*, *Katsuwonus*, *Thunnus*). These species inhabit a wide range of
395 environmental conditions in marine ecosystems. Tuna species can be found in coastal and
396 oceanic pelagic waters, and have wide geographic distributions, ranging from the tropics to
397 higher temperate latitudes with some degree of habitat partitioning by depth. Tropical tuna
398 species can spawn throughout the year, while the subtropical and temperate tunas undergo
399 seasonal migrations back to warm waters for spawning (Juan-Jordá et al 2013, Horswill et al
400 2019). Paleoceanographic evidence suggests that ancestral tunas evolved in a tropical
401 environment approximately 60 million years ago (Monsch 2000) and over time they have
402 diversified and evolved a suite of morphological and physiological adaptations that have allowed

them to expand their distributions into more temperate environments or deeper colder waters where they can encounter higher prey densities to support their high somatic and gonadal growth rates (Dickson and Graham 2004). Reflecting their tropical ancestor, all tunas (except for the slender tuna *Allothunnus fallai*) spawn in warm waters, requiring a sea surface temperature of at least 24 °C (Schaefer 2001). This is a key aspect of their reproductive biology that we include in our model scenarios.

To connect our mechanistic model more explicitly with the observed patterns of life history variation in tunas, we followed a proposed categorization of tunas into three ecological lifestyles, (Bernal et al. 2017). The three general lifestyles are based on species-specific vertical, latitudinal, and temporal (seasonal) distributions and movement patterns of tunas (Figure 3; Bernal et al. 2009, Bernal 2011, Bernal et al. 2017). The first ecological lifestyle represents a tuna species that largely remain within the warmer and well-oxygenated surface layer above the thermocline (generally above 20 °C) during both day and night. These tuna species have limited vertical movements as they do not descend below the thermocline (Figure 3). Coastal species, such as the tropical frigate tuna *(Auxis thazard)* may typify this group. The second ecological lifestyle represents tuna species that spend the majority of the time above the thermocline (generally above 20 °C) but also visit depths below the thermocline for foraging (Figure 4). The oceanic species of yellowfin tuna (*Thunnus albacares*) with year-round tropical distributions typifies this group. Its vertical movement exposes this species to a wider range of temperatures and to less-oxygenated waters at depth but only for short periods of time because this species is not hypoxia tolerant (Schaefer et al. 2009). The third ecological lifestyle characterizes tuna species that are exposed to a wider range of environmental conditions and spend significant

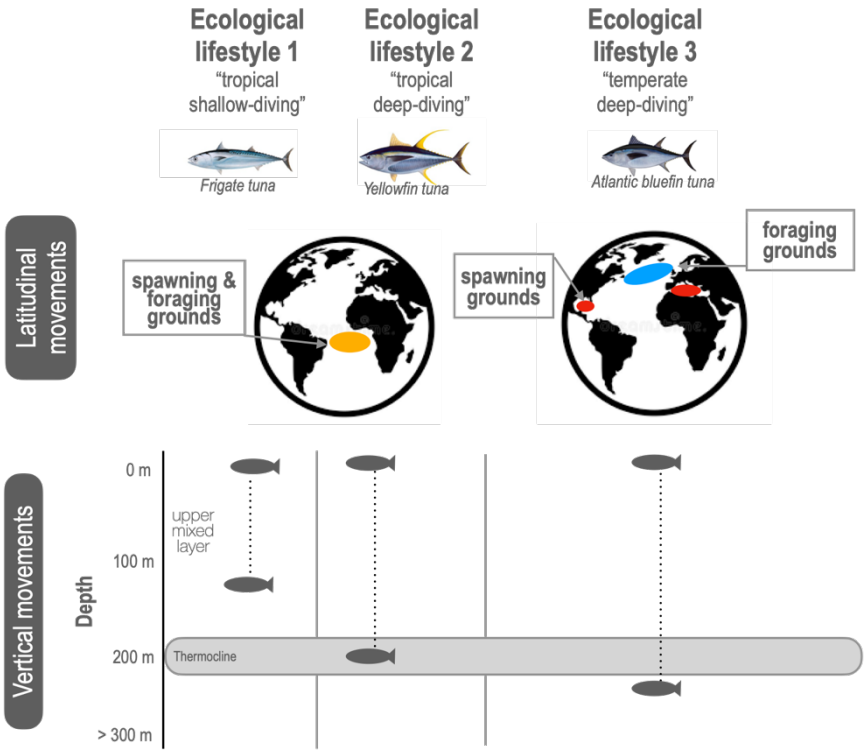

Figure 3. Three representative ecological lifestyles of tunas and their distribution patterns based on their latitudinal and vertical movements. Characteristic spawning and foraging grounds are shown for each lifestyle; examples are the tropical shallow-diving frigate tuna *Auxis thazard*, tropical deep-diving yellowfin tuna *Thunnus albacares,* and temperate deep-diving Atlantic bluefin tuna *Thunnus thynnus*. Fish silhouettes represent the depth distribution where species spend most of their time. The thermocline is defined as the depth range within which the water temperature changes rapidly and separates the water column into the upper well-mixed surface layer (water above 20 °C) and the deeper waters (waters below 15 °C). Figure modified from Bernal et al. 2009 and Bernal et al 2017.

periods of time in colder waters (Figure 3). The oceanic and temperate Atlantic bluefin tuna (*Thunnus thynnus*) are one species that typifies this group, spending most of the year at higher

latitudes in colder and more productive waters between the upper mixed later and the cooler deep waters below the thermocline, and migrating to warmer waters for spawning (Bernal et al. 2017).

To examine whether our model could predict these three broad ecological lifestyles of tunas, we modelled environmental scenarios corresponding to each lifestyle in terms of temperature, ecosystem productivity, and seasonality. We chose parameters based on the results of our general model., but also added seasonal fluctuations in temperature to represent the bluefin tuna migration from temperate, productive waters to their tropical spawning grounds. We then asked whether the traits emerging in these scenarios matched the range of reported sizes of three representative species corresponding to each lifestyle (Juan-Jordá et al. 2016).

Sensitivity analyses

We ran a series of tests to examine how our choices of parameters in the size spectrum influence model predictions. Specifically, we varied values of h (representing efficiency in prey capture or hunger levels) in the predation function (Eq. 3) and φ (the fraction of body mass that can be devoted to reproduction) in the reproductive constraint (Eq. 10). We also conducted sensitivity analyses in which we varied the scale and shape coefficients in the metabolic cost function (c and θ, respectively, in Eq. 5). Motivated by our tuna case study, we also varied seasonality in resources, temperature, and spawning. We considered seasonal environments in which only resources and only temperature varied, to understand how these factors alone contributed to observed variation in body size and reproductive output. We additionally considered growth and reproductive patterns with an expanded the warm season (where individuals could spawn in warm temperatures for six months of the year, instead of three). Finally, we determined in

preliminary analyses that the maximum lifespan T did not strongly affect model results, because most individuals reach a maximum body size well before the final time T.

Results

Our model produces age-specific relationships between body size (length, from which we calculate mass using Eq. 6) and reproduction that correspond to a range of fish life histories. In general, we found that individuals allocated energy to growth early in life and shifted this allocation to reproduction in later life. An asymptotic growth pattern naturally emerged from the model, after a period of exponential growth early in life (Fig. 4A). Ecosystem productivity (κ) alone generated a range of maximum body sizes, from less than 100 cm at low levels of productivity to well over 350 cm (Fig. 4A). Across scenarios of ecosystem productivity, the predicted trajectories for individual growth were identical in early life. However, growth slowed earlier in lower productivity environments (Fig. 4A). For all life histories, allocation to reproduction began at very low levels sometime during the individual's second year (Fig. 4B) and increased steadily as the individual aged until it reached a maximum. Both the rate at which reproduction increased with size and the maximum reproductive output were consistently greater with increased ecosystem productivity (Fig. 4B). We also found the pattern of age-specific mortality was very similar in early life for all productivities κ, but that lifespan increased predictably as asymptotic body size increased (Supp. Fig. 5).

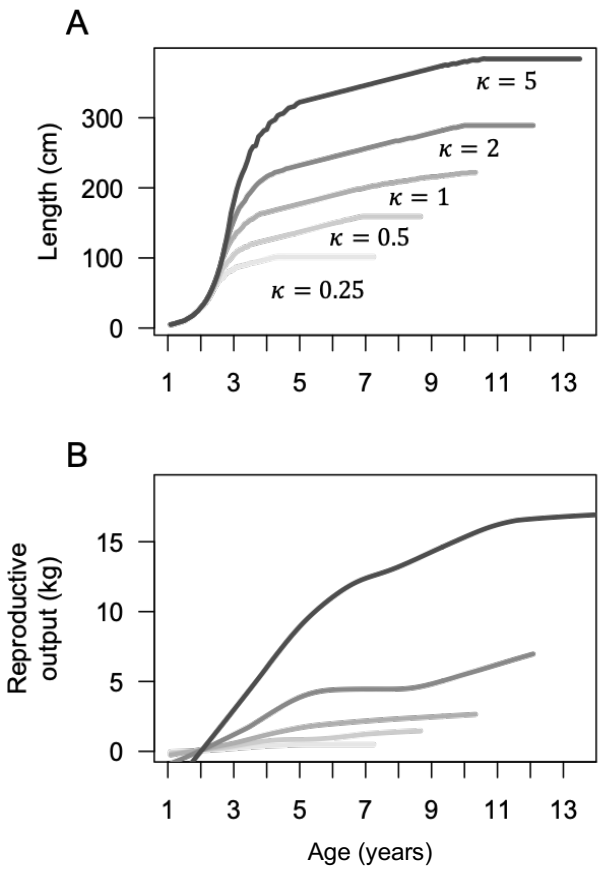

Figure 4. (A) Growth (size at age) and (B) Expected reproductive output of individuals in different productivity κ scenarios. Each curve ends when an individual's expected survival chances are less than 3%. Temperature in every scenario was constant at 16.85 ℃, and h was constant at 8. The reproductive output was smoothed using the loess tool in R; data points can be found in Supp. Fig. 4.

When we compared the interacting effects of ecosystem productivity (κ) and environmental temperature (τ) on patterns of growth and reproductive allocation, we found the effects of temperature on body size and reproductive output were relatively small (Fig. 5). The biggest differences emerged in highly productive environments with dramatic increases in temperature. Specifically, when average temperature increased by 10 degrees (e.g., from 11.85 to 21.85 ℃ or from 16.85 to 26.85 ℃), maximum body sizes were 3-10% smaller, with the largest differences occurring when $\kappa = 5$ (specific values in Fig. 5 are reported in Supp. Table 1). At the same time, these increases in temperature led to concomitant reductions in lifetime reproductive output that ranged from 3-10% (Fig 5B). However, it is important to note that comparing thermal increases

in 5-degree intervals only generated minor (3- 5%) decreases in growth and reproduction, unless both predators and prey were scarce ($\kappa \leq 0.5$, Supp. Table 1).

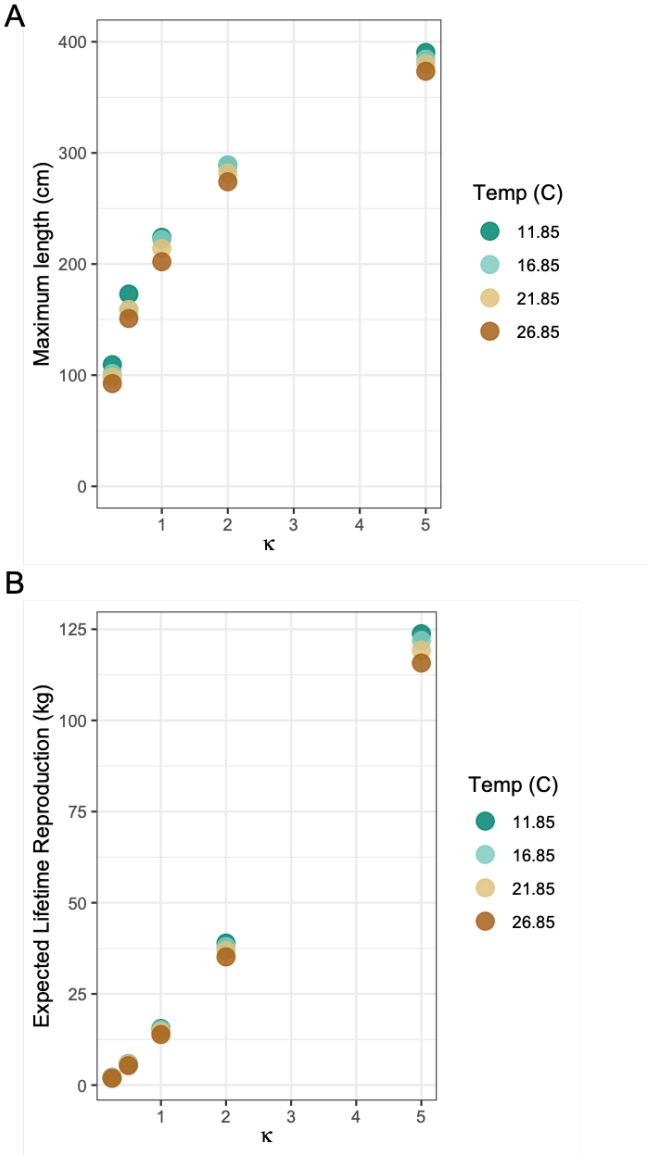

Figure 5. (A) Maximum body size and (B) Expected lifetime reproductive output (in kg) of individuals plotted against a range of productivity scenarios. Color of points corresponds to differences in average annual temperature in °C.

The interacting effects of temperature and productivity on body size suggests that when both prey and predators are abundant, the benefits of growing large outweigh associated increases in metabolic costs. We also found the effect of temperature on survival was indirectly expressed through body size, i.e., where temperature influenced asymptotic body size (Fig. 5A) it had a

488 predictable effect on lifespan. In other words, when individuals reduced growth and remained
489 smaller in thermally taxing conditions to avoid being unable to meet their energetic requirements
490 for maintenance, it equates to an increased risk of predation and thus shorter lifespans. In
491 sensitivity analyses, we varied the parameter *h,* representing predator efficiency or hunger level
492 (Eq. 3; Andersen 2019), to change the allometric properties of the risk of predation (Supp. Fig.
493 6). However, while varying this parameter affected the realized lifespans, it did not dramatically
494 change individual growth trajectories or patterns of size-specific reproduction (Supp. Fig. 6).
495 By contrast, the constraint on the amount of lipid stores that can be spent each month on
496 reproduction, φ, was of more importance for growth because it depends directly on the
497 individual's structural mass. This parameter contributes biological realism to the state dynamics,
498 but is difficult to measure or estimate directly, especially for fish that spawn multiple times per
499 year, because often little is known about the frequency of spawning. In sensitivity analyses, we
500 found that making this constraint more stringent (e.g., decreasing φ from 0.2 to 0.1) led to
501 increased body sizes at both high and low productivity values (Supp. Fig. 7).
502
503 One of our aims is ultimately to address the life history variation observed in tunas, so
504 throughout we used estimates of parameters for the metabolic cost function that were measured
505 experimentally for tuna species (Clarke and Johnston 1999). However, to understand if the
506 relatively small effect of increased temperatures on body size in Figure 5 is robust to differences
507 in physiological costs, we conducted sensitivity analyses in which the shape and allometric
508 scaling of costs varied (Supp. Figs. 8 and 9). We confirmed that our choice of parameters for this
509 function had relatively minor influences on growth and reproduction (consistent with the effect
510 of temperature), with the exception of an extreme scenario when the cost scaling coefficient *c*

increased by a factor of 10 (Supp. Fig. 9). This outlier scenario confirms that our model is working correctly (i.e., it is possible to eventually find thermal costs severe enough to change our results), but that our estimates for the parameterization of metabolic costs are unlikely to be unrealistically biasing our broader conclusions.

The growth, body size, and reproductive patterns that emerged in three environmental scenarios corresponding to each of the three tuna lifestyles outlined in Fig. 3 qualitatively matched the life history of each representative species (Figure 6, Table 2). In the environmental scenario representing the tropical shallow-diving lifestyle, we predicted individual body sizes of less than 100 cm. Less than 3% of individuals survived past 10 years of age and they reproduced continuously at relatively low levels (left column, Figure 6). These predicted traits are similar to those of frigate tuna *Auxis thazard,* a tropical shallow-diving tuna species with small body size. In the environmental scenario matching the tropical deep-diving lifestyle, we predicted growth to sizes well over 200 cm, lifespans of less than 15 years, and continuous reproductive output that increases over the individual's life (middle column, Figure 6, Table 2). While we believe this is consistent with the life histories of tropical deep-diving tuna species such as yellowfin tuna *Thunnus albacares*, lifetime reproductive patterns of these batch-spawning species are not well known (Horswill et al. 2019). In the environmental scenario matching the lifestyle of temperate deep-diving tunas, such as Atlantic bluefin tuna, *Thunnus thunnus,* we predicted the maximum body sizes exceeded 350 cm and individuals were predicted to live much longer than 18 years (right column, Figure 6, Table 2). Spawning was constrained to be seasonal in tunas in the third ecological lifestyle (i.e., spawning could only occur in temperatures above 24 ℃, which we specified individuals experienced for three months of the year).

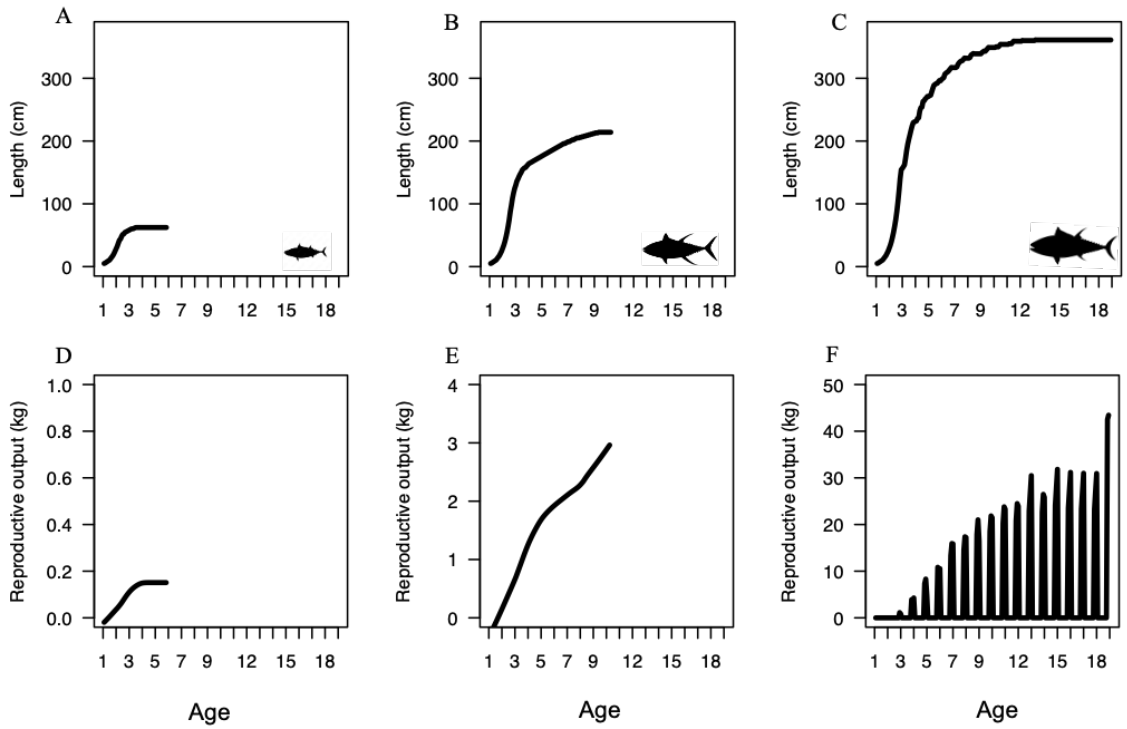

Figure 6. Growth (top row) and reproduction (bottom row) predicted by our model in each of the three representative environmental scenarios corresponding to the three ecological lifestyles of tunas (columns). With the exception of C and F, all curves end at the age when less than 3% of the population is expected to survive, representing the cohort lifespan. A and D represent tropical shallow-diving tuna species such as the frigate tuna *Auxis thazard*. B and E represent tropical deep-diving tuna species such as yellowfin tuna *Thunnus albacares*. C and F represent temperate deep-diving species such as Atlantic bluefin tuna *Thunnus thynnus*, which migrate seasonally from higher latitudes with colder and productive waters to less productive and warmer waters. At age 18, more than 10% of individuals in the temperate deep-diving lifestyle were still alive and are likely to live much longer (C,F). As in Fig. 4, the reproductive output in panels D-E was smoothed using the loess function. Parameters are found in Table 2.

Analysis of seasonality in temperature and spectrum productivity.

The results of the tuna case study yielded an unexpected pattern: when environmental temperature and ecosystem productivity varied seasonally, individuals grew to be 14% larger than the size observed constant scenarios that are otherwise comparable in terms of productivity (κ) and temperature (τ) (Figure 5; Supp. Table 2). To investigate the differential effects of seasonality in temperature (in which species spawn for three months in waters that are 9 degrees warmer than their winter foraging grounds) and in productivity (which increases threefold during winter months), we conducted several follow-up comparisons. In Figure 7 we plot a range of values for average productivity and the body size and reproduction patterns that emerge in different seasonality scenarios. Specifically, we compared four scenarios across a range of ecosystem productivities: (i) the scenario when temperature increased during the spawning season but productivity did not change (ii) a threefold increase in productivity for nine months (with constant temperature throughout the year) (iii) three months of seasonality in both temperature and productivity (as in Fig. 6C,F), (ii) predictions from the constant scenario when τ = 16.85 ℃ (from Fig. 5).

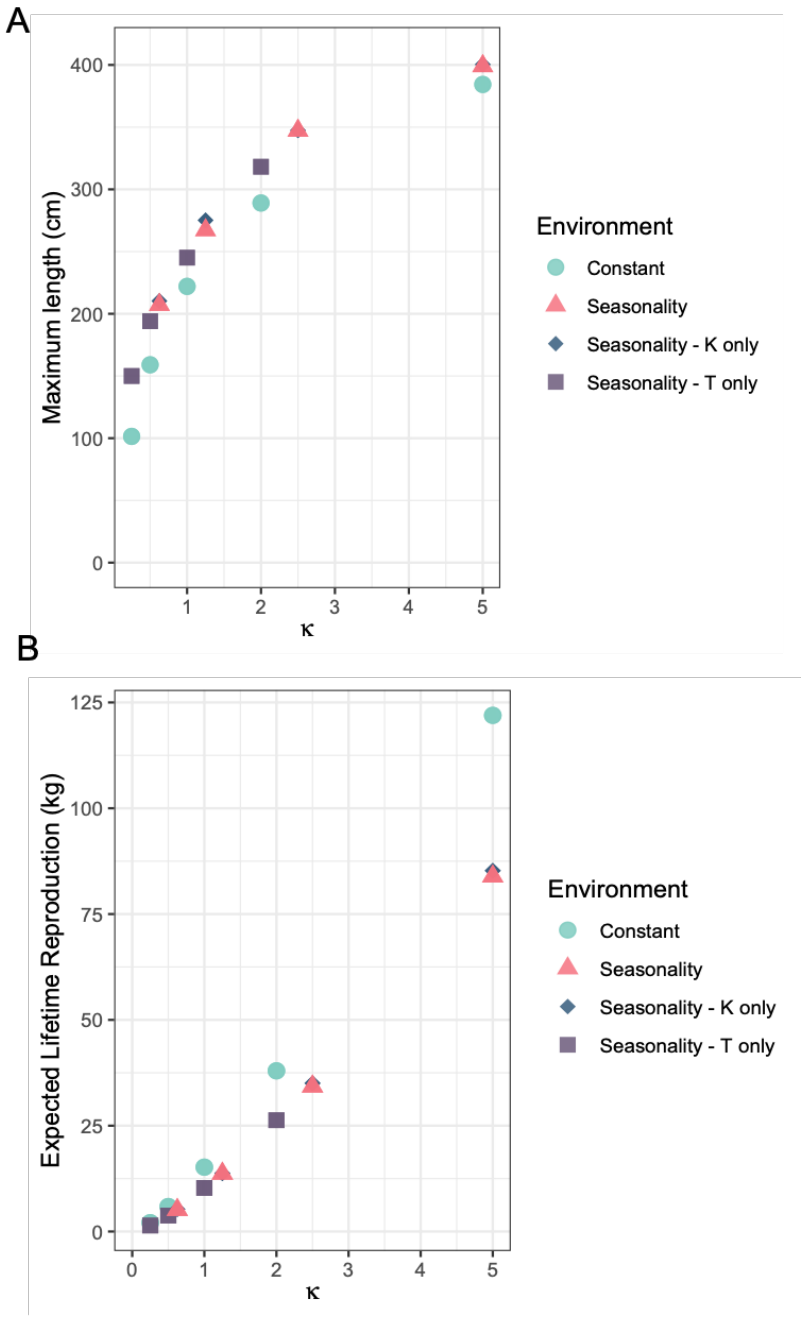

Figure 7. (A) Maximum body size and (B) Expected lifetime reproductive output (in kg) of individuals plotted in different scenarios of seasonality in spawning, temperature, and productivity. In each scenario, the cool season or baseline temperature was 16.85 °C. In all three seasonal scenarios, spawning activity was limited to three months.

Figure 7 illustrates that the pattern of increased body size in seasonal environments (relative to constant environments) and consistent increases in length of 12-16% are predicted for a range of seasonality and productivity scenarios (Supp. Table 2). Scenarios with increased temperature or increased productivity alone led to larger body sizes, comparable to the increase expected in the

fully seasonal scenario (Fig. 7A). In Supp. Table 2 we report specific values of body length for different productivity and seasonality combinations to illustrate effects of temperature and productivity alone are consistently comparable to those when combined. Expected lifetime reproduction is markedly lower in seasonal environments when spawning is limited to three months of the year. From this set of analyses, we infer that resources and temperature effects on energetic budgets are not the primary drivers of larger body sizes in our model. Rather, the compression of reproductive opportunities into three months of the year, and the temporal separation of reproduction from the most valuable foraging opportunities, favors increased allocation to growth overall. To further understand this effect, we varied spawning season length and reproductive constraints. In Supp. Fig 10 we compare body sizes in environments in which spawning seasons lasted six months (i.e., warmer temperatures and reduced foraging opportunities lasted twice as long). We also modelled seasonality in resources and temperature, while allowing reproduction to occur year-round. When individuals spawned in warm, low productivity ecosystems for six months instead of three, asymptotic body lengths were smaller. Furthermore, when reproduction was unconstrained, but individuals experienced warm, low productivity conditions for three months of the year, body sizes were again smaller and comparable to the scenario with seasonality in spawning for six months (Supp Fig. 10).

Discussion

Changes in environmental temperature and ecosystem productivity have been occurring for decades and have been shown to affect fish recruitment, growth, and fishery productivity (Free et al. 2019; Oke et al. 2020). There have been several mechanisms proposed to explain these

581 changes (Fernandes et al. 2020). Early models based on physiology predicted that increased
582 temperature will lead to reduced growth and smaller body sizes (Cheung et al. 2008), yet have
583 been countered by recent experimental evidence showing growth is less affected by temperature
584 than reproductive allocation (Wootton et al. 2022), and that metabolic rate can adapt to increased
585 temperatures (Pilakouta et al. 2020). Physiological models have ignored ecological interactions
586 because it has been challenging to represent and evaluate the effects of the food- and fearscape
587 upon somatic growth. To address this gap, we developed a general model incorporating insights
588 from size spectra theory to parametrize the risk of predation (fearscape) and the availability of
589 prey (foodscape) for individuals of different sizes. We predicted emergent body sizes and
590 reproductive and mortality patterns in the context of ecosystem food web interactions,
591 represented by size spectra.
592
593 Here, we introduce and approach integrating community processes, including size-specific
594 foraging success and predation risk, into a model of individual fitness. Our model and results
595 build on prior models of life history traits grounded in energy budgets (Ejsmond et al. 2010;
596 Jusup et al 2011) in which increased allocation to reproduction leads to a slowdown in growth
597 rate with age. Alternatively, asymptotic growth patterns have been predicted by physiological
598 models that broadly assume surface uptake areas, relative to the volume of metabolically
599 available mass, leads to intrinsic geometric constraints causing asymptotic growth (von
600 Bertalanffy 1960, Pauly 2010). In our model, multiple (mainly extrinsic) ecological mechanisms
601 led to slowing of growth and emergence of an asymptotic size in each environment. Notably,
602 unlike previous models, in our models the onset of reproduction alone does not correspond
603 immediately to decreasing growth rates and explain where asymptotic body sizes emerge.

Instead, the availability of prey, physical and temporal limits on resource intake, the risk of predation, and constraints on gonad size and reproductive timing all increase the advantage of growing to larger body sizes; these advantages are balanced against metabolic demands and the actual energetic requirements of growth.

Consistent with expectations, our model predicted larger maximum body sizes, greater reproductive output, and longer lifespans when resources were plentiful; by contrast, in less productive ecosystems, individuals were small, with shorter lifespans. Across a range of temperatures, the benefits of growing large through the foodscape and fearscape outweighed the increase in metabolic costs until very large sizes or very dramatic increases in temperature. For example, although our model predicted smaller body sizes and decreased lifetime reproduction at higher temperatures when both predators and prey were scarce, these differences were relatively small until average temperatures increased by 10-15 ℃. Ecosystem productivity κ had a much stronger influence on our results than any of our other parameters. One exception came when estimating age-specific mortality of each environment, which was more sensitive to our choice of the value representing variation due to predator satiation or efficiency in prey capture (*h,* Eq. 3). However, this process did not substantially change growth trajectories.

We used variation among tuna ecological lifestyles as a motivation for our model parameterizations and comparisons, while also aiming to provide general insights. We successfully predicted growth patterns that are consistent with species representing each ecological lifestyle (Fig. 6). Unexpectedly, we found an effect of seasonal variation on body size, where individuals grew larger when they experienced higher productivity or colder

627 temperatures for part of the year (but average productivities were similar). Further investigation
628 revealed this effect is present with seasonal variation in temperature or in productivity alone, and
629 that these effects were not additive nor interactive (Fig. 7, Supp. Table 2), which rules out
630 explanations based on metabolic costs and strongly supports the conclusion that growth is driven
631 by the limited time available for reproduction, coupled with the opportunity to forage and store
632 energy, but not reproduce, the rest of the year. These results could explain giantism in polar
633 environments. For fishes like tunas, which often exhibit a combination of capital and income
634 breeding, and for which reproduction is determined by temperature, warmer conditions will
635 eventually allow spawning at higher latitudes for longer periods. Our results suggest that
636 cascading effects on their growth are not easily predicted and will depend on how warming
637 waters reverberate through the size spectrum.
638
639 Our model illustrates that predicting responses in growth and reproduction in changing
640 environments is complex, because optimal strategies responding to selective pressures from
641 many factors, including constraints on storage and reproduction, physiology, and the nature of
642 ecosystem fearscapes and foodscapes. For the analyses presented here, we have assumed a static
643 relationship between length and mass, and the conversion of mass to joules (energy density of
644 tissue). Keeping these relationships constant ensured a common currency linking individual
645 energetic budgets to ecological changes in predation risk and foraging success. Exploring the
646 consequences of these relationships for differences among clades would be a natural follow-up to
647 our study. For example, while we did not directly address the interaction between of fisheries
648 induced selection and growth, it is a rich area of further investigation (Audzijyonte et al. 2016).
649 Plastic or evolutionary responses to fishing potentially include faster growth, earlier maturation

rates, and smaller maximum body sizes, but the consequences for marine food webs are complex (Hočevar and & Kuparinen 2021). The framework introduced here potentially could capture how eco-evolutionary feedbacks between fishing mortality, growth and mass relationships, and ecosystem size spectra interactively affect trends in body sizes of focal species. Studies of the interaction between fishing and size spectra have been focused on lake systems where food webs have been studied in greater detail (Perälä and Kuparinen 2020). Understanding how these physiological and ecological processes are linked is necessary to understand how species will respond to different environmental changes and climate change scenarios; our findings suggest that when predicting future growth patterns under projected changes in climate, several ecological and physiological factors will play a greater role than temperature in determining trends in body size.

Appendix. Optimization details.

Dynamic programming equations (Eq. 14) are constrained optimization algorithms with the purpose of determining the optimal set of behaviors or decisions that maximize a quantitative metric over time, such as lifetime expected reproductive success. A key property is that the decisions at one time affect the state variables at the next time. When solving Eq. 14, we consider how the allocation decisions an individual makes during one month of its life affect its future size, energetic reserves (lipid stores) and chances of survival, and find the set of allocation to growth and reproduction that maximizes its fitness in a given environment. We are able to calculate lifetime fitness by solving the equation using backwards iteration. By starting at $t = T - 1$, and assuming there is no possibility of future fitness (i.e., the second term of Eq. 14 is

equal to zero for all possible values of length and lipid stores) we can populate the array with the fitness of all possible combinations of length, lipid stores, and allocation strategies at $t = T - 1$; this fitness will be the first term on the right side of Eq. 14. This process is repeated, working backwards, until $t = 1$. We can thereby determine the combination of g and r that maximizes both current fitness at t, and the fitness expected from $t + 1$ until T, given the chance of survival, length, and lipid stores (the future states in Eq. 12) resulting from that particular strategy. Solving Eq. 14 in this way produces an array storing the proportional allocation to growth and reproduction that leads to the highest lifetime fitness, for all possible combinations of size and lipid stores (l and s) for every month until the final time T.

Solving a dynamic programming equation with two state variables, such as Eq. 14, is computationally expensive, and we employed a number of techniques to make the iteration more efficient and to approximate a smooth fitness surface. First, we constrained the parameter space that was evaluated. Specifically, we used an integer index I (with a maximum of I_{max}) to represent lipid stores s, converting the index to values in joules in the dynamic loop. We then related the range of s we explored to each value of l (because lipid stores are constrained by l), by setting

$$s = \frac{0.6 \cdot I^3 \rho a {l_{max}}^3}{{I_{max}}^3}$$

In other words, we adjusted the numerical step size for possible values of s to be finer for smaller individuals. Furthermore, we used linear interpolation of state values (Clark and Mangel 2000) when computing expected future fitness in Eq. 14 to minimize discontinuities on the fitness landscape arising from the integer index of energetic state. We did not interpolate length, since

its unit (centimeters) was sufficiently fine-grained that there were minimal effects of discontinuities.

All programming was done using R 4.1.1 and all code and model outputs will be available. We ran the code to solve the dynamic programming equation and simulate the individual life histories using Rscript commands from the Linux shell of a 2019 MacPro with 16 cores and 96 GB of RAM. Jobs were run in parallel and the runtime of each job was between 60 and 120 minutes. The results of each job are presented in the figures summarizing growth, reproduction, and survival data; these analyses and figures were produced in the Rstudio IDE.

References

Andersen, K. H. 2019. *Fish Ecology, Evolution, and Exploitation: A New Theoretical Synthesis.* Princeton University Press, Princeton.

Andersen, K. H., Jacobsen, N. S., Farnsworth, K. D., and J. Baum. 2016. The theoretical foundations for size spectrum models of fish communities. *Canadian Journal of Fisheries and Aquatic Sciences* 73:575–588.

Audzijonyte, A., Fulton, E., Haddon, M., Helidoniotis, F., Hobday, A.J., Kuparinen, A., Morrongiello, J., Smith, A.D., Upston, J. and Waples, R.S., 2016. Trends and management implications of human-influenced life-history changes in marine ectotherms. *Fish and Fisheries*, *17*(4), pp.1005-1028.

Audzijonyte, A., Richards, S.A., Stuart-Smith, R.D., Pecl, G., Edgar, G.J., Barrett, N.S., Payne, N. and Blanchard, J.L., 2020. Fish body sizes change with temperature but not all species shrink with warming. *Nature Ecology & Evolution*. 4:809-814.

Audzijonyte, A. and Richards, S.A., 2018. The energetic cost of reproduction and its effect on optimal life-history strategies. *American Naturalist*. 192:E150-E162.

Audzijonyte, A., Jakubavičiūtė, E., Lindmark, M., and Richards S.A. 2022 Mechanistic Temperature-Size Rule Explanation Should Reconcile Physiological and Mortality Responses to Temperature. *The Biological Bulletin* 2022 243:2, 220-238

Barnes, W., Maxwell, D., Reuman, D.C., and Jennings, S., 2010. Global patterns in predator-prey size relationships reveal size dependency of trophic transfer efficiency. *Ecology* 91:222-232.

Benoît, E., and M. J. Rochet. 2004. A continuous model of biomass size spectra governed by predation and the effects of fishing on them. *Journal of Theoretical Biology* 226:9-21.

Bernal, D. 2011. Physiological specializations of different fish groups. Pelagic fishes. Pages 1887-1902 *in* Farrell AP (ed) *Encyclopedia of Fish Physiology: From Genome to Environment,* Vol 3. Academic Press, San Diego.

Bernal, D., Sepulveda C., Musyl, M., Brill, R. (2009) The eco- physiology of swimming and movement patterns of tunas, billfishes, and large pelagic sharks. Pages 436–483 *in* Domenici P, Kapoor BG (eds) *Fish Locomotion: an Etho-Ecological Approach*. Science Publishers, Enfield.

Bernal, D., Brill, R.W., Dickson, K.A. and H.A. Shiels. 2017. Sharing the water column: physiological mechanisms underlying species-specific habitat use in tunas. *Reviews in Fish Biology and Fisheries* 27:843-880.

Bernhardt, J.R., Sunday, J.M. and M.I. O'Connor. 2018. Metabolic theory and the temperature-size rule explain the temperature dependence of population carrying capacity. *American Naturalist.* 192:687-697.

Beverton, R. J. H., and S. J. Holt. 1959. A review of the lifespans and mortality rates of fish in nature, and their relation to growth and other physiological characteristics. Pages 142–177 *in* CIBA Foundation Colloquium on Ageing.

Bigman, J.S., M'Gonigle, L., Wegner, N.C. and Dulvy, N.K. 2021. Respiratory capacity is twice as important as temperature in driving patterns of metabolic rate across the vertebrate tree of life. *Science Advances* 7: eabe5163.

Blanchard, J. L., Heneghan, R. F., Everett, J. D. , Trebilco, R. and A. J. Richardson. 2017. From bacteria to whales: using functional size spectra to model marine ecosystems. *Trends in Ecology & Evolution.* 32:174-186.

Blanchard, J. L., Jennings, S., Law, R., Castle, M.D., McCloghrie, P., Rochet, M.J., and E. Benoît. 2009. How does abundance scale with body size in coupled size-structured food webs? *Journal of Animal Ecology*. 78:270-280.

Blanchard, J.L., Jennings, S., Holmes, R., Harle, J., Merino, G., Allen, J.I., Holt, J., Dulvy, N.K. and M. Barange. 2012. Potential consequences of climate change for primary production and fish production in large marine ecosystems. *Phil. Trans. Roy. Soc. B* 367:2979-2989.

Brown, J. H., J. F. Gillooly, A. P. Allen, V. M. Savage, and G. B. West. 2004. Toward a metabolic theory of ecology. *Ecology.* 85:1771-1789.

Chapman, E. W., Kørgensen, C., and M. E. Lutcavage. 2011. Atlantic bluefin tuna (*Thunnus thynnus*): a state-dependent energy allocation model for growth, maturation, and reproductive investment. *Canadian Journal of Fisheries and Aquatic Sciences* 68:1934–1951.

Charnov, E. L., Berrigan, D., and R. J. H. Beverton. 1991. Dimensionless numbers and the assembly rules for life histories. *Phil. Trans. Roy. Soc. B* 332:41-48.

Charnov, E. L., and J. R. Krebs. 1974. On clutch-size and fitness. *Ibis.* 116:217-219.

Cheung, W.W., Close, C., Lam, V., Watson, R., and D. Pauly 2008. Application of macroecological theory to predict effects of climate change on global fisheries potential. *Marine Ecology Progress Series*. 365:187-197.

Christensen, A. and Andersen, K.H., 2011. General classification of maturation reaction-norm shape from size-based processes. Bulletin of Mathematical Biology, 73(5): 1004-1027.

Cichoń, M. and Kozłowski, J., 2000. Ageing and typical survivorship curves result from optimal resource allocation. Evolutionary Ecology Research, 2(7): 857-870.

Clark, C. W., and M. Mangel. 2000. Dynamic state variable models in ecology: methods and applications. Oxford University Press, Oxford.

Clarke, A. 2006. Temperature and the metabolic theory of ecology. *Functional Ecology* 20:405-412.

Clarke, A., and N. M. Johnston. 1999. Scaling of metabolic rate with body mass and temperature in teleost fish. *Journal of Animal Ecology*. 68: 893-905.

Conover, D. O., and S. B. Munch. 2002. Sustaining fisheries yields over evolutionary timescales. *Science* 297:94–96.

Daufresne, M, Lengfellner, K., and U. Sommer. 2009. Global warming benefits the small in aquatic ecosystems. *Proc. Nat. Acad. Sci.* 106:12788–12793.

Dickson, K.A., and Graham, J.B. 2004. Evolution and consequences of endothermy in fishes *Physiological and Biochemical Zoology* 77: 998-1018.

Ejsmond, M.J., Czarnołęski, M., Kapustka, F. and Kozłowski, J., 2010. How to time growth and reproduction during the vegetative season: an evolutionary choice for indeterminate growers in seasonal environments. *The American Naturalist* 175(5): 551-563.

Fernandes, J.A., Rutterford, L., Simpson, S.D., Butenschön, M., Frölicher, T.L., Yool, A., Cheung, W.W. and Grant, A., 2020. Can we project changes in fish abundance and distribution in response to climate? *Global Change Biology.* 26:3891-3905.

Free, C.M., Thorson, J.T., Pinsky, M.L., Oken, K.L., Wiedenmann, J. and Jensen, O.P. 2019. Impacts of historical warming on marine fisheries production. *Science.* 363: 979-983.

Froese R. 2006. Cube law, condition factor and weight-length relationships: history, meta-analysis and recommendations. *Journal of Applied Ichthyology* 22: 241-253

Gadgil, M., and W. H. Bossert. 1970. Life historical consequences of natural selection. *American Naturalist* 104:1-24.

Giacomini, H.C., Shuter, B.J. and Lester, N.P., 2013. Predator bioenergetics and the prey size spectrum: Do foraging costs determine fish production? *Journal of Theoretical Biology* 332: 249-260.

Gillooly, J. F., Brown, J. H., West, G. B., Savage, V. M., and E. L. Charnov. 2001. Effects of size and temperature on metabolic rate. *Science.* 293:2248–2251.

Gislason, H., Daan, N. Rice, J. C., and J. G. Pope. 2010. Size, growth, temperature and the natural mortality of marine fish. *Fish and Fisheries* 11:149–158.

Hilborn, R. and Mangel, M. 1997. *The Ecological Detective.* Princeton University Press, Princeton, NJ.

Hočevar, S., & Kuparinen, A. (2021). Marine food web perspective to fisheries-induced evolution. *Evolutionary Applications*, 14, 2378– 2391.

Horswill, C., H. K. Kindsvater, M. J. Juan-Jordá, N. K. Dulvy, M. Mangel, and J. Matthiopoulos. 2019. Global reconstruction of life-history strategies: A case study using tunas. *Journal of Applied Ecology* 56:855-865.

Houston, A., C. Clark, J. McNamara, and M. Mangel. 1988. Dynamic Models in Behavioural and Evolutionary Ecology. *Nature.* 332:29-34

Houston, A., and J. McNamara. 1999. *Models of Adaptive Behaviour*. Cambridge University Press.

Hulthén, K., Hill, J.S., Jenkins, M.R. and Langerhans, R.B., 2021. Predation and resource availability interact to drive life-history evolution in an adaptive radiation of livebearing fish. *Frontiers in Ecology and Evolution*, 9, p.619277.

Jørgensen, C., K. Enberg, and M. Mangel. 2016. Modelling and interpreting fish bioenergetics: a role for behaviour, life-history traits and survival trade-offs. *Journal of Fish Biology* 88:389–402.

Jørgensen, C., and Ø. Fiksen. 2006. State-dependent energy allocation in cod (*Gadus morhua*). *Canadian Journal of Fisheries and Aquatic Sciences* 63:186–199.

Juan-Jordá, M. J., I. Mosqueira, J. Freire, and N. K. Dulvy. 2013. The Conservation and Management of Tunas and Their Relatives: Setting Life History Research Priorities. *PLoS ONE* 8:e70405.

Juan-Jordá, M.J., Mosqueira, I., Freire, J., Ferrer-Jordá, E. and Dulvy, N.K. 2016. Global scombrid life history data set. *Ecology*, 97: 809-809.

Jusup, M., Klanjscek, T., Matsuda, H., Kooijman, S.A.L.M. 2011. A Full Lifecycle Bioenergetic Model for Bluefin Tuna. *PLoS ONE* 6(7): e21903.

Kindsvater, H.K., Alonzo, S.H., Mangel, M. and Bonsall, M.B., 2010. Effects of age-and state-dependent allocation on offspring size and number. *Evolutionary Ecology Research*, 12(3), pp.327-346.

Kingsolver, J. G., and R. B. Huey. 2008. Size, temperature , and fitness: three rules. *Evolutionary Ecology Research* 10:251–268.

Kiørboe, T., and A. G. Hirst. 2014. Shifts in mass scaling of respiration, feeding, and growth rates across life-form transitions in marine pelagic organisms. *American Naturalist* 183:E118-E130.

Kitchell, J.F., Neill, W.H., Dizon, A.E., and J.J. Magnuson. 1978. Bioenergetic Spectra of Skipjack and Yellofin Tunas. In:Sharp, G.D., Dizon, A.A. (Eds.), *The Physiological Ecology of Tunas.* Academic Press.

Kozłowski, J., 1992. Optimal allocation of resources to growth and reproduction: implications for age and size at maturity. *Trends in Ecology and Evolution*, 7(1):15-19.

Kozlowski, J. 1996. Optimal allocation of resources explains interspecific life-history patterns in animals with indeterminate growth *Proc. R. Soc. B.* 263: 559-566.

Kozłowski, J. and Teriokhin, A.T., 1999. Allocation of energy between growth and reproduction: the Pontryagin Maximum Principle solution for the case of age-and season-dependent mortality. *Evolutionary Ecology Research* 1(4): 423-441

Law, R., M. J. Plank, A. James, and J. L. Blanchard. 2009. Size-spectra dynamics from stochastic predation and growth of individuals. *Ecology* 90:802-811.

Lika, K. and Kooijman, S.A., 2003. Life history implications of allocation to growth versus reproduction in dynamic energy budgets. Bulletin of Mathematical Biology, 65(5), pp.809-834.

Oke, K.B., Cunningham, C.J., Westley, P.A.H., Baskett, M.L., Carlson, S.M., Clark, J., Hendry, A.P., Karatayev, V.A., Kendall, N.W., Kibele, J. ,Kindsvater, H.K., Kobayashi, K.M., Lewis, B., Munch, S., Reynolds, J.D., Vick, G.D., and E.P. Palkovacs. 2020. Recent declines in salmon body size impact ecosystems and fisheries. *Nature communications*, 11:1-13.

Perälä, T, Kuparinen, A. Eco-evolutionary dynamics driven by fishing: From single species models to dynamic evolution within complex food webs. *Evol Appl*. 2020; 13: 2507– 2520.

Perrin, N. and Sibly, R.M., 1993. Dynamic models of energy allocation and investment. Annual Review of Ecology and Systematics, 24: 379-410.

Perrin, N., Sibly, R.M. and Nichols, N.K., 1993. Optimal growth strategies when mortality and production rates are size-dependent. Evolutionary Ecology, 7(6), pp.576-592.

Mangel, M. 2006. The Theoretical Biologist's Toolbox : Quantitative Methods for Ecology and Evolutionary Biology. Cambridge University Press.

Mangel, M. 2015. Stochastic dynamic programming illuminates the link between environment, physiology, and evolution. *Bulletin of Mathematical Biology* 77:857-877.

Mangel, M. and C. W. Clark. 1988. *Dynamic Modelling in Behavioral Ecology.* Princeton University Press, Princeton.

Monsch, K.A. 2000 *The Phylogeny of the Scombroid Fishes.* PhD thesis, University of Bristol p 272.

Neubauer, P., and K. H. Andersen. 2019. Thermal performance of fish is explained by an interplay between physiology, behaviour and ecology. *Conservation Physiology* 7:coz025

Pauly D. 2010. Gasping fish and panting squids: oxygen, temperature and the growth of water-breathing animals. International Ecology Institute, Germany.

Pilakouta, N, Killen, SS, Kristjánsson, BK, et al. 2020. Multigenerational exposure to elevated temperatures leads to a reduction in standard metabolic rate in the wild. *Funct Ecol*. 34:1205-1214.

Pignalosa, P., Pappalardo, L., Gioacchini, G., Carnevali, O. 2020. Length-weight relationships and a new length conversion factor for Atlantic Bluefin tuna (*Thunnus thynnus L.*) caught in the Mediterranean Sea. *Collect. Vol. Sci. Pap. ICCAT,* 76(2): 138-146.

Quince, C., Abrams, P.A., Shuter, B.J. and Lester, N.P., 2008. Biphasic growth in fish I: theoretical foundations. *Journal of Theoretical Biology*, 254(2): 197-206.

Schaefer, K.M. 2001. Reproductive biology of tunas. *Fish Physiology.* 19: 225-270.

Schaefer K.M., Fuller D.W., and B.A. Block 2009. Vertical movements and habitat utilization of skipjack (*Katsuwonus pelamis*), yellowfin (*Thunnus albacares*), and bigeye (*Thunnus obesus*) tunas in the Equatorial Eastern Pacific Ocean, ascertained through archival tag data. Pages 121-144 *in* Nielsen, J.L., Arrizabalaga, H., Fragoso, N., Hobday, A., Lutcavage, M., Sibert, J. (Eds.), *Tagging and Tracking of Marine Animals with Electronic Devices*. Springer, New York.

Sheldon, R.W., Prakash, A. and Sutcliffe Jr., W.H. 1972. The distribution of particles in the ocean. *Limnology and Oceanography.* 17:327-340.

Sheldon, R.W., Sutcliffe Jr., W.H., and M.A. Paranjape. 1977. Structure of pelagic food chain and relationship between plankton and fish production. *Journal of the Fisheries Research Board of Canada*. 34: 2344-2353.

Shuter, B.J., Giacomini, H.C., de Kerckhove, D. and Vascotto, K., 2016. Fish life history dynamics: shifts in prey size structure evoke shifts in predator maturation traits. *Canadian Journal of Fisheries and Aquatic Sciences*. 73(4): 693-708.

Southwood, T.R.E. 1977. Habitat, the Templet for Ecological Strategies? *Journal of Animal Ecology*. 46:337-365.

Sprules, W. G., and L. E. Barth. 2016. Surfing the biomass size spectrum: some remarks on history, theory, and application. *Canadian Journal of Fisheries and Aquatic Sciences* 73:477-495.

Thygesen, U.H., Farnsworth, K.D., Andersen, K.H., Beyer, J.E. 2005. How optimal life history changes with the community size-spectrum. *Proc. R. Soc. B*. 272:1323-1331.

Trebilco, R., Baum, J. K., Salomon, A. K., and N. K. Dulvy. 2013. Ecosystem ecology: Size-based constraints on the pyramids of life. *Trends in Ecology & Evolution*. 28:423-431.

Ursin, E. 1973. On the prey size preferences of cod and dab. *Meddelelser fra Danmarks Fiskeri- og Havundersøgelser* 7: 85–98.

Varpe, Ø., 2017. Life history adaptations to seasonality. *Integrative and comparative biology*, *57*(5), pp.943-960.

von Bertalanffy L. 1960. Principles and theory of growth. Pages 137-259 *in* Nowinski, W.W., Ed., *Fundamental Aspects of Normal and Malignant Growth*, Elsevier, Amsterdam.

Walsh, M. R., and D. N. Reznick. 2009. Phenotypic diversification across an environmental gradient: a role for predators and resource availability on the evolution of life histories. *Evolution* 63:3201–3213.

White, C.R., Alton, L.A., Bywater, C.L., Lombardi, E.J. and Marshall, D.J., 2022. Metabolic scaling is the product of life-history optimization. *Science*, *377*(6608), pp.834-839.

Wong, S., Bigman, J.S., and N.K. Dulvy. 2021. The metabolic pace of life histories across fishes. *Proc. R. Soc. B.* 288:20210910.

Wootton, H.F., Morrongiello, J.R., Schmitt, T. & Audzijonyte, A. 2022. Smaller adult fish size in warmer water is not explained by elevated metabolism. Ecology Letters, 25, 1177– 1188.

Yanco, S.W., Pierce, A.K. and Wunder, M.B. 2022. Life history diversity in terrestrial animals is associated with metabolic response to seasonally fluctuating resources. Ecography. 2022:e05900

1009 **Table 1**. Description of parameters and variables

Parameter or Variable	Description	Value
w	Body mass in kg	-
N	Number of individuals in a size category (or trophic level) when considering a Sheldon size spectrum	-
B	Absolute biomass in a size category (or trophic level) when considering a Sheldon size spectrum	-
κ	The spectrum parameter, which defines the total biomass of organisms of the smallest body size w in a given ecosystem; Andersen (2019) gives an estimate of 10 gained by averaging over all Predator-Prey Mass Ratio estimates measured from gut contents. We vary it to represent ecosystem differences in overall ecosystem richness	Varies
$Bprey$	Biomass of prey expected by a focal individual	-
μ_p	Instantaneous risk of mortality due to predation, which depends on body mass and position in the size spectrum	-
h	Predation risk, comprised of predator satiation estimates (estimated from gut contents) and predator preference (or effectiveness) for consuming prey of a given mass (Andersen 2019)	4, 8
τ	Temperature of the environment (in degrees Kelvin except where noted)	285-300
C	Metabolic requirements (costs) that scale with mass and temperature	-
c	Normalization constant scaling metabolic costs (in J), based on metabolic rate data from tunas (Kitchell et al. 1978)	5×10^{16}
k_B	Boltzmann constant, relating particle energy to temperature in units of m^2 kg s^{-2} K^{-1}	1.3×10^{-23}
E	The average activation energy for the rate limiting enzymes in metabolism in units of joules; from the metabolic theory of ecology (Gillooly et al. 2001).	1.04×10^{-19}
θ	Metabolic scaling exponent; values vary among clade, here we use a value reported for tunas (Clarke and Johnston 1999)	0.66
ρ	The energy density of tuna body mass in our model in J/kg (estimated empirically and reported in Chapman et al. 2011)	4.2×10^{6}
t	Time in monthly time steps in the dynamic model	-
T_{max}	Maximum lifespan in months	216
l, $L(t)$	Body length (in cm) This is a dynamic state variable but can only increase with time. The maximum value possible is 400 cm. For a specific value, we use the capital letter notation.	-
s, $S(t)$	Lipid stores (in joules) – this is a dynamic state variable representing energy stores that can be used for metabolism, growth, and reproduction.	-
a	Scale coefficient relating length to structural mass, similar to values estimated empirically for bluefin tuna and reported in Pignalosa et al. (2020).	1.0×10^{-5}
$w(t)$	Structural mass of the individual (in kg) at time t – this depends on $L(t)$	-
υ	The fraction of structural mass that determines the critical threshold of energetic mass needed for survival	0.1
φ	The fraction of structural mass that determines the maximum possible reproductive output in a monthly time step	0.2
γ_{pred}	Survival from predation from one month to the next	
γ_s	Survival, given that the individual has sufficient energy reserves to meet metabolic requirements and avoid starvation	
g	Proportion of lipid stores allocated to growth (this allocation decision is optimized by the dynamic programming equation); can take values between 0 and 1	
r	Proportion of lipid stores allocated to reproduction (this allocation decision is optimized by the dynamic programming equation); can take values between 0 and 1 and the sum of g and r cannot exceed one.	
$R(l,s,t)$	Current fitness, the product of lipid stores and the optimal allocation to reproduction, r	
$V(l,s,t)$	Expected accumulated lifetime reproduction from time t onwards, given that $L(t) = l$ and $S(t) = s$	

1010
1011
1012
1013

Table 2

Parameter values for environmental scenarios corresponding to the three ecological lifestyles of tunas described in Fig. 3, with corresponding predicted body size and maximum observed fork length (cm) for three representative species (data from Juan-Jordá et al. 2016).

Lifestyle	**Environment**	**Baseline or winter temp**	**Yearly mean κ**	***h***	**Predicted body size**	**Representative species**	**Reported range of body sizes**
Tropical shallow	Constant	26.85 C	0.1	8	62 cm	Frigate tuna	40-60 cm
Tropical deep diving	Constant	21.85 C	1	8	214 cm	Yellowfin tuna	125-231 cm
Temperate deep diving	Seasonal	11.85	2.5	12	361 cm	Bluefin tuna	203-427 cm

Supplemental Table 1. Model outputs corresponding to points in main text Figure 6. All scenarios had constant environments.

Temperature τ in ℃	κ	Lifetime reproductive output (kg)	Maximum body length (cm)
11.85	0.25	2.15	109.5
11.85	0.5	5.87	173
11.85	1	15.51	224
11.85	2	38.94	289.1
11.85	5	123.77	390.4
16.85	0.25	2.08	101.5
16.85	0.5	5.9	159
16.85	1	15.2	222
16.85	2	37.97	289
16.85	5	121.95	384.3
21.85	0.25	2.02	98.4
21.85	0.5	5.65	159
21.85	1	14.73	214
21.85	2	36.93	282
21.85	5	119.28	380.3
26.85	0.25	1.85	92.4
26.85	0.5	5.33	151
26.85	1	13.85	202
26.85	2	35.15	274
26.85	5	115.73	373.4

Supplemental Table 2. Precise values for body lengths predicted in varying seasonality scenarios for the same value of average κ. These data are complementary to Figure 7, where scenarios that are constant or have seasonality in τ have a different average productivity κ. The differences between different seasonal scenarios at lower average productivity (κ = 1.25) disappear at higher average productivity (κ = 2.5). This suggests that the multiple factors leading to the optimization of the growth-reproduction tradeoffs make the fitness landscape more complex when productivity is lower.

Environment	κ	Length (cm)
Constant	1.25	238.1
Seasonality - κ only	1.25	275.2
Seasonality - τ only	1.25	272.2
Seasonality	1.25	267.3
Constant	2.5	305.1
Seasonality - κ only	2.5	347.4
Seasonality - τ only	2.5	347.4
Seasonality	2.5	347.2

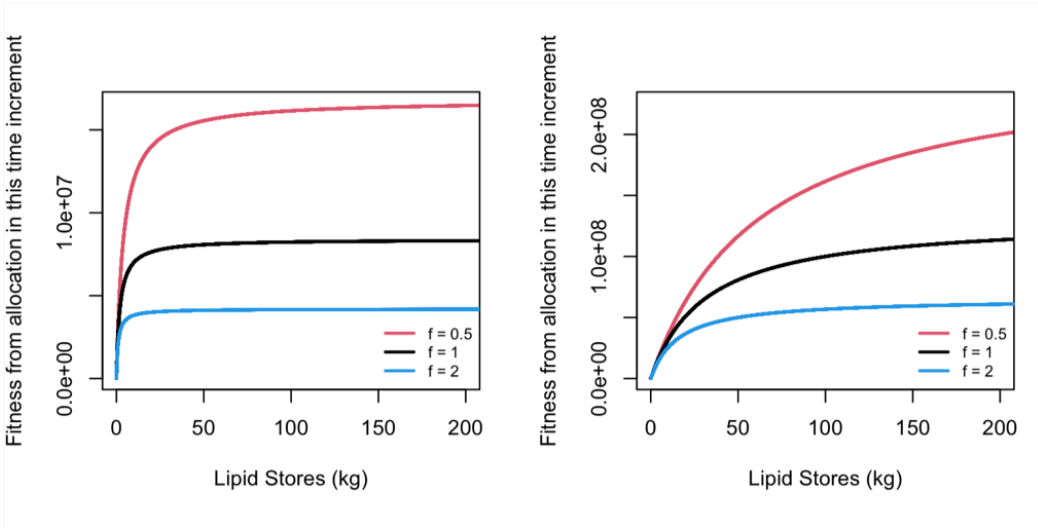

Supplementary Figure 1. The fitness increment expected with different amounts of lipid reserves (energy stores) Left panel: Fitness increment for an individual of 100 cm. Right panel: Fitness increment for an individual of 250 cm. We show the shape of the function for three values of *f* but for all analyses here we used *f* = 1.

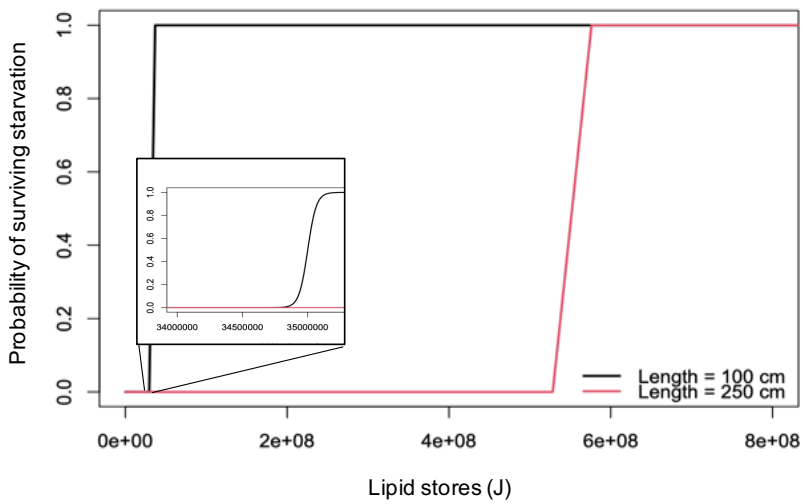

Supplementary Figure 2. Main panel: The sigmoid relationship between lipid stores (in joules) and survival for individuals of different lengths. The threshold amount of energy required for metabolic maintenance is a fixed proportion of body mass. The probability of avoiding starvation $\gamma_s(s, l)$ is a logistic function of mass given in Eq. 13. Inset: closeup of the x-axis in the region encompassing the smaller threshold.

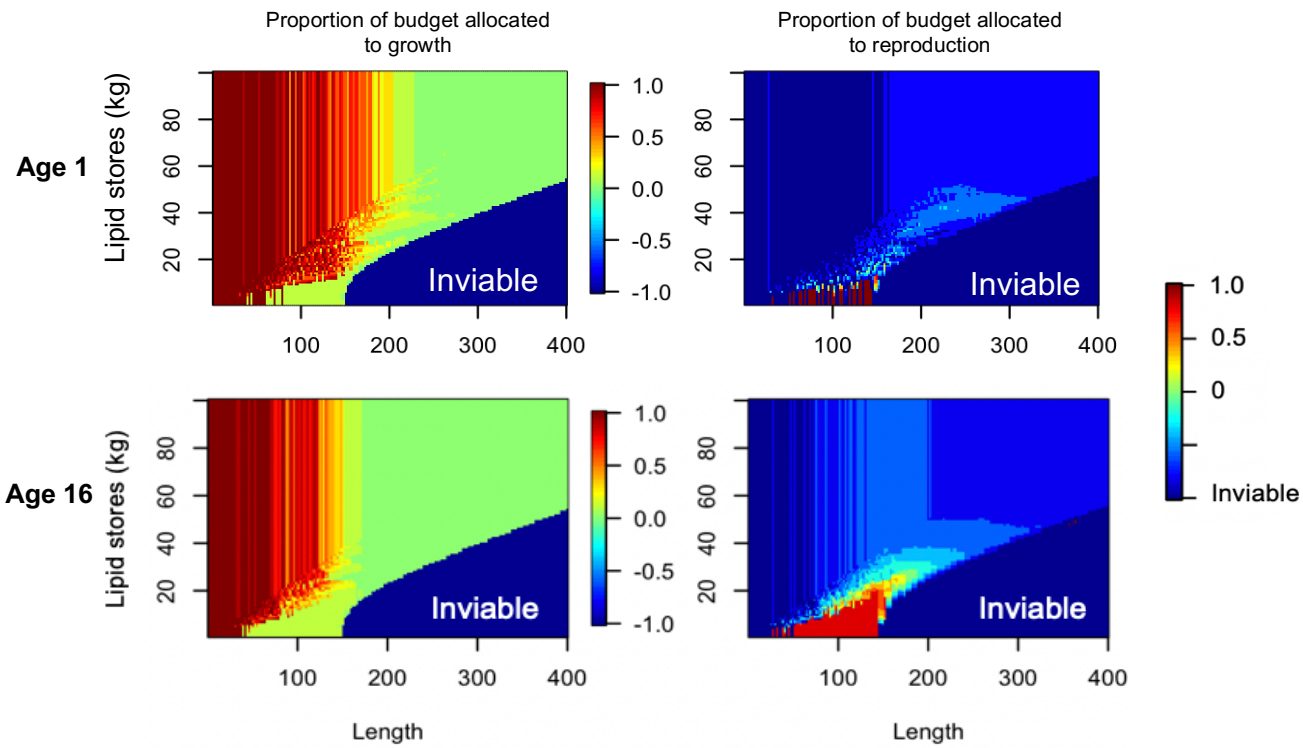

Supplementary Figure 3. Example rules for allocation to growth and reproduction for ages 1 and 16. The inviable region (dark blue) represents parameter space where remaining stores are insufficient for survival, given the individual's length (in other words, energetic requirements for maintenance are not met). Comparing panels within rows shows differences between allocation to growth and reproduction as a function of state and length. Comparing panels within columns shows how the tradeoff between growth and reproduction changes with age. Note that the striations come from the discretization of allocation values of g and r in Eq. 14.

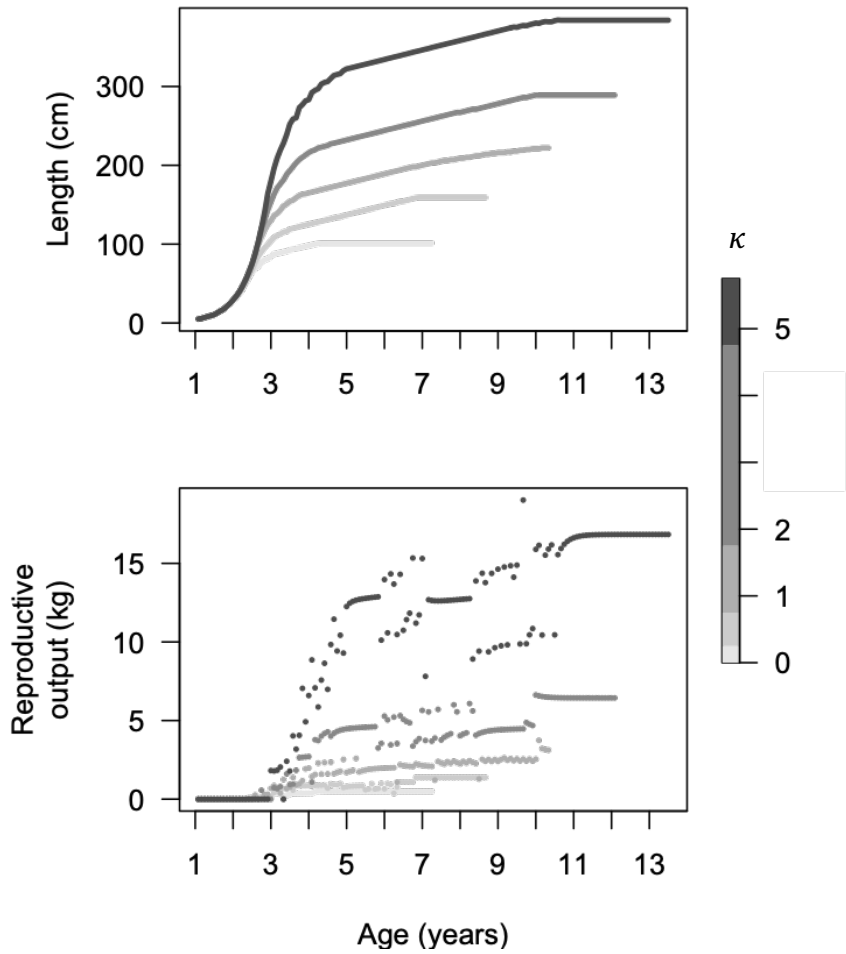

Supplementary Figure 4. Top: The emergent pattern of survival to age at different levels of κ. Bottom: The natural log of survival to age. Dashed horizonal line shows the cutoff past which less than 3% of individuals will survive. For all results here, h = 8 and $\tau = 16.85$℃

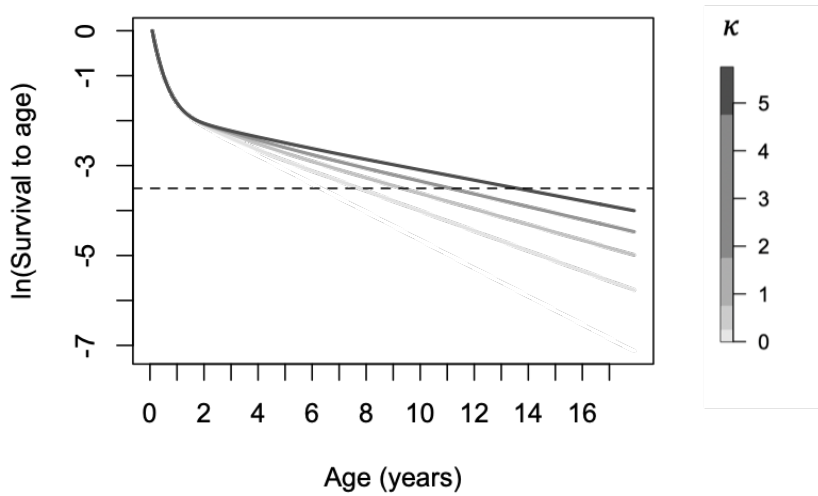

Supplementary Figure 5. The emergent pattern of ln(survival) to age at different levels of κ. Dashed horizonal line shows the cutoff past which less than 3% of individuals will survive. For all results here, h = 8 and $\tau = 16.85$°C.

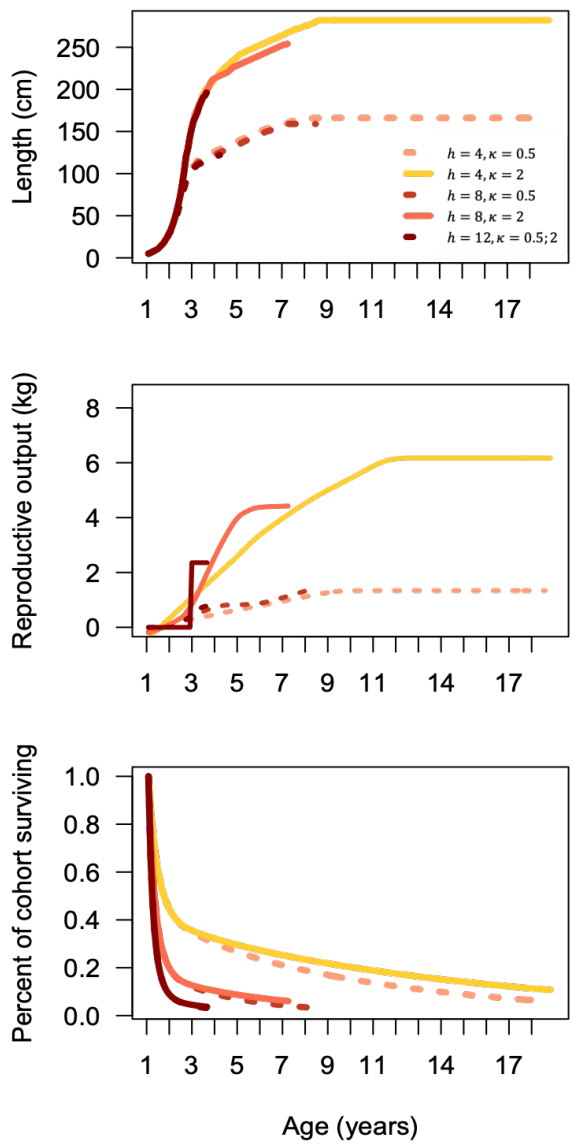

Supplementary Figure 6. The emergent patterns of growth, reproduction, and survival that emerge when h varies. We contrast two values of κ to highlight that it is still the main driver of variation in body size, although h affects lifespan. In all scenarios, $\tau = 16.85°C$. Note that for results presented elsewhere, $h = 8$ except where noted.

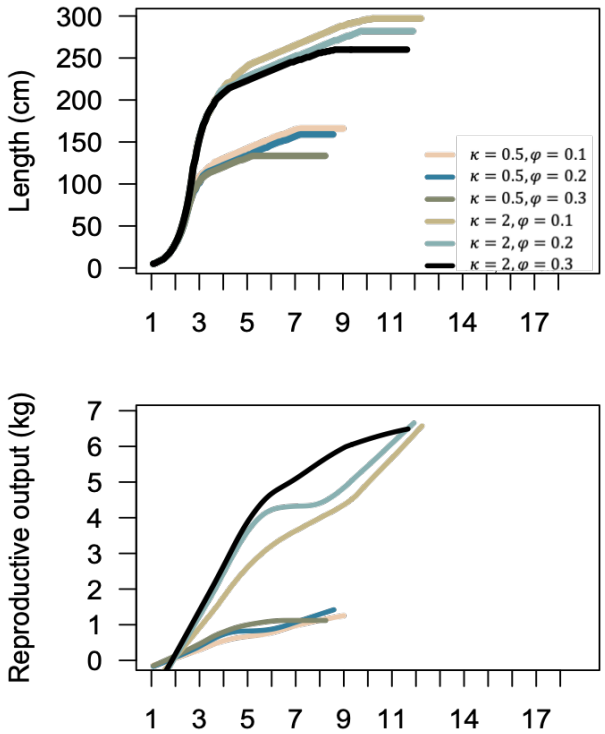

Supplementary Figure 7. Growth curves showing the effect of changes in the reproductive capacity φ, for two values of κ. As the reproductive constraint increases (the fraction of the body cavity that can be devoted to gonad decreases from 0.2 to 0.1), selection favors the evolution of larger body sizes. In all scenarios, $\tau = 16.85$℃. Note that for all results presented elsewhere, $\varphi = 0.2$.

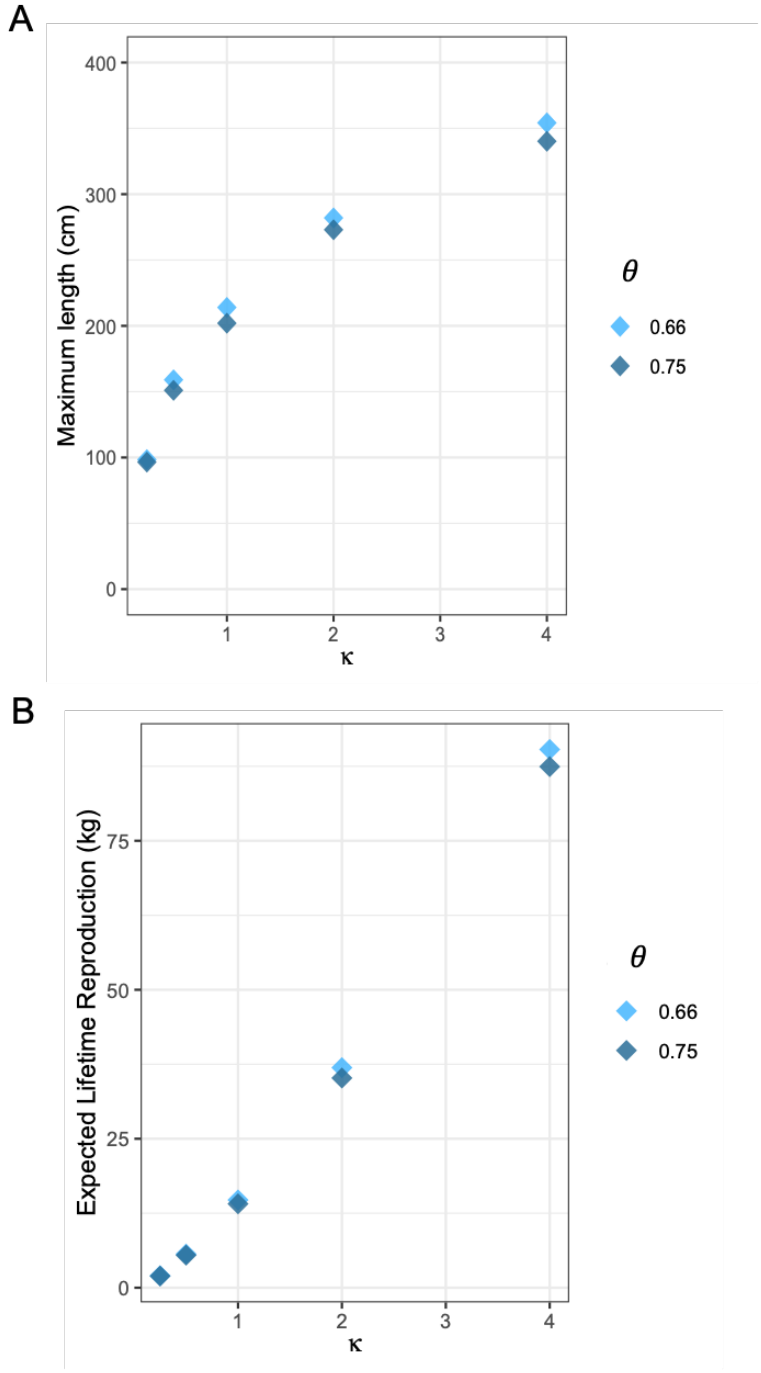

Supplementary Figure 8. Body size and lifetime reproduction for several values of κ and θ (the allometric exponent in the metabolic cost function). For all scenarios, temperature is constant year-round at 21.85°C.

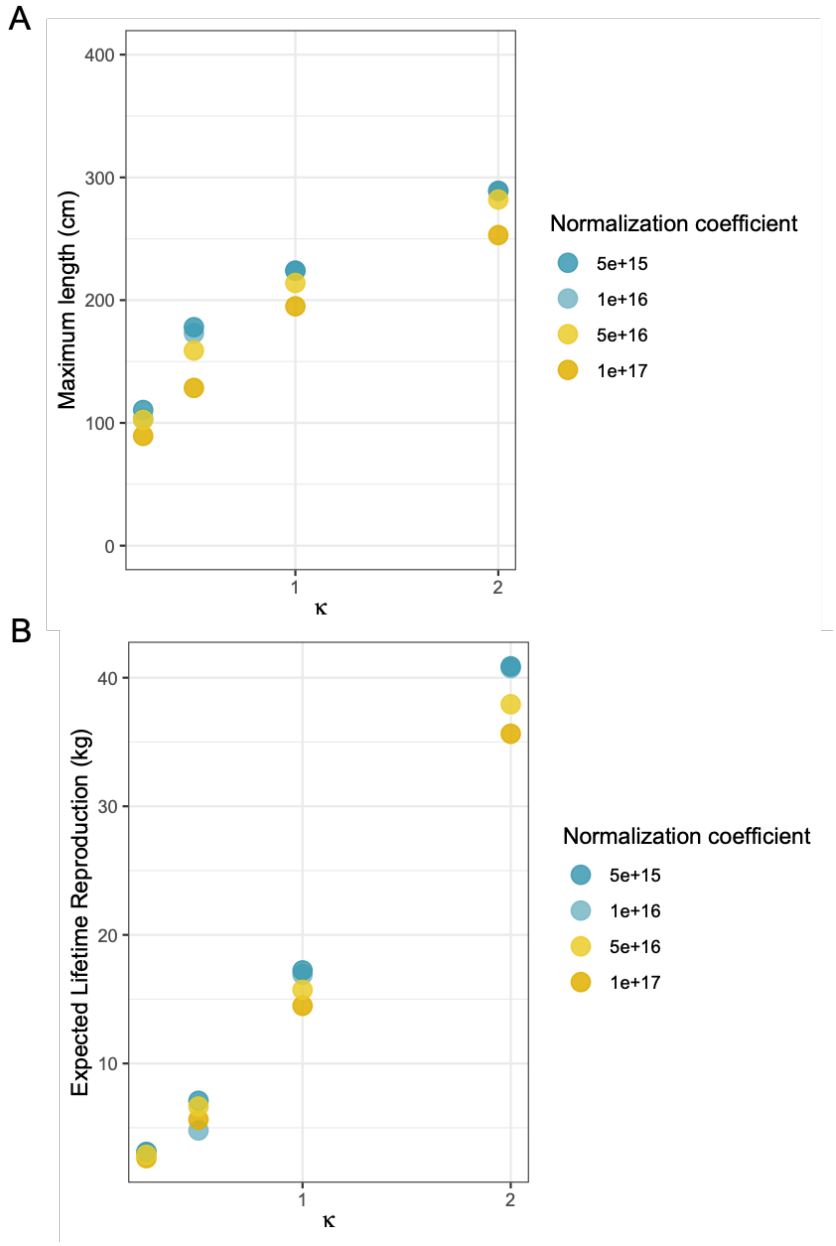

Supplementary Figure 9. Body size and lifetime reproduction for several values of κ and c (the normalization constant in the metabolic cost function). The estimate of c used elsewhere (5×10^{16}) comes from metabolic rate data from tunas (Clarke and Johnston 1999). For all scenarios, temperature is constant year-round at 21.85°C.

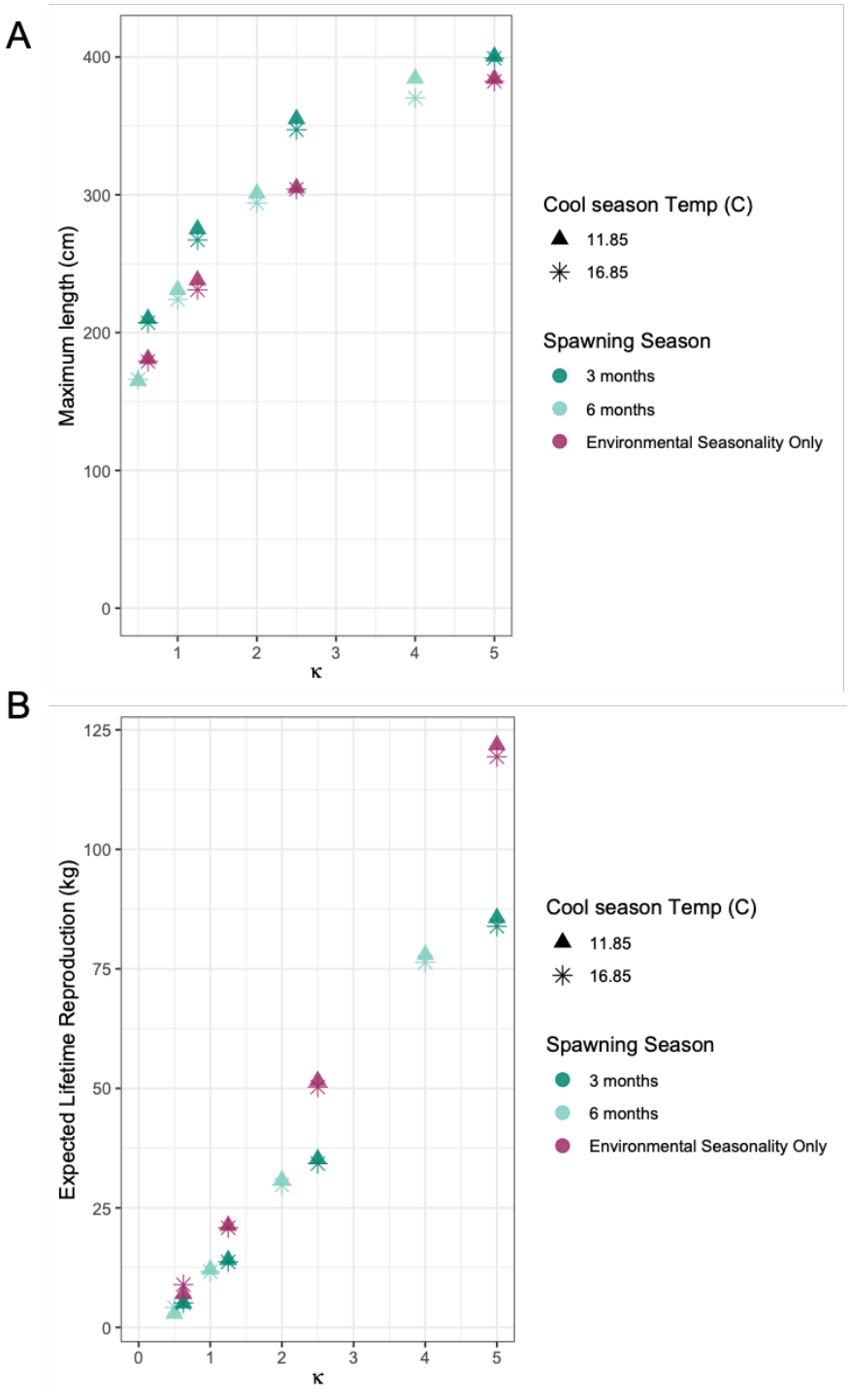

Supplementary Figure 10. Body size and lifetime reproduction for several values of κ and temperature, and three scenarios of spawning season duration. Note that the darker teal stars (corresponding to a three-month spawning season and a winter temperature of 16.85°C) match the fully seasonal scenario in the main text Fig. 7. Magenta points correspond to the scenario where individuals can spawn year-round.